NASA Contractor Report 144884

TESTING AND ANALYSIS OF DUAL-MODE ADAPTIVE LANDING GEAR, TAXI MODE TEST SYSTEM FOR YF-12A

Max A. Gamon

September 1979

NASA

NASA Contractor Report 144884

TESTING AND ANALYSIS OF DUAL-MODE ADAPTIVE LANDING GEAR, TAXI MODE TEST SYSTEM FOR YF-12A

Max A. Gamon
Lockheed-California Company
Burbank, California

Prepared for
Dryden Flight Research Center

National Aeronautics and
Space Administration

1979

TABLE OF CONTENTS

LIST OF FIGURES

LIST OF FIGURES (Continued)

LIST OF TABLES

CONVERSION TABLE, U.S. TO S.I. UNITS

U.S. Units	X Conversion	= S.I. Units
Pounds	4.448	Newtons
Pounds/Inch	175.1	Newtons/Meter
Pounds/Square Inch	6895.	Pascal
Inch	0.0254	Meter
Foot	0.3048	Meter
Cubic Inches	1.639×10^{-5}	Cubic Meters

TESTING AND ANALYSIS OF DUAL-MODE ADAPTIVE LANDING GEAR, TAXI MODE TEST SYSTEM FOR YF-12A

Max A. Gamon
Lockheed-California Company

SUMMARY

The purpose of this program is to determine the effectiveness of a dual-mode adaptive landing gear system in reducing the dynamic response of an airplane during ground taxiing. In addition, the test program provides a data base that is useful for determining the degree of correlation between analytically predicted dynamic taxi responses and test results. The test results were obtained using the NASA YF-12A research airplane (S/N 935) operating on Runway 04-22 at Edwards Air Force Base. The dual-mode system is a landing gear system in which a relatively flat air curve is used for taxiing, and a conventional air curve is used for landing impact.

The program results indicate that the dual-mode system as tested provides dynamic taxi response reductions of 25 percent at the cg and 30 to 45 percent at the cockpit. Lesser response reductions are observed at other locations on the airplane. Pilot comments indicate that the degree of ride improvement is quite noticeable, particularly at the higher gross weights. Analytical results using a digital computer program to model the test taxi conditions yield excellent correlation with test data at the airplane cg, and good correlation at other airplane locations with the exception of the cockpit, which exhibits poor correlation between test and analytical results. The analytical studies indicate the significant contribution of the airplane normal vibration modes to the response time histories, and the importance of using accurate normal modes.

INTRODUCTION

The objectives of this study are to determine the effectiveness of a dual-mode adaptive landing gear system (DMS) in reducing the dynamic response of an airplane during ground taxiing, and to ascertain the degree of correlation attainable between analytically predicted dynamic taxi responses and actual test results. The test results were obtained with the NASA YF-12A instrumented research airplane (S/N 935), operating on Runway 04-22 at Edwards Air Force Base.

The DMS is a landing gear system in which a relatively flat air curve is used for ground operations, and a conventional air curve is used for landing impact. Since most landing gears are optimized for the landing impact condition, the air curve used is effective in minimizing landing impact dynamic loads. However, the resulting air curve is generally somewhat stiffer than ideal for isolation from runway roughness during taxiing. Figure 1 illustrates a typical main gear load-deflection air curve, labeled "landing", and a flatter air curve labeled "taxiing". With the DMS, the airplane lands on the landing curve, and after the initial impact is absorbed, the air curve transitions to the taxiing curve. This curve is then used for all subsequent ground operations, including the next takeoff. During flight, the system returns to the landing curve to complete the cycle.

The method of implementing the DMS is discussed in Reference 1. Since the purpose of this study is to examine the effectiveness of the flat air curve for taxiing, no attempt is made to evaluate the entire system as described in Reference 1. For the taxi tests with the YF-12A, a simplified ground-test version of the DMS was employed. The only hardware required was an air bottle connected to each landing gear air-servicing port with a 0.5-inch O.D. line. The bottles were mounted in close proximity to the gear so that the interconnecting line lengths were 20 inches or less. The combination of the added volume of the air bottle and an increased, fully extended gear pressure results in the flatter load-deflection air curve as shown in Figure 1. Since the gear stiffness at a given load level is just the slope of the load-deflection air curve, the flatter air curve corresponds to a softer landing gear.

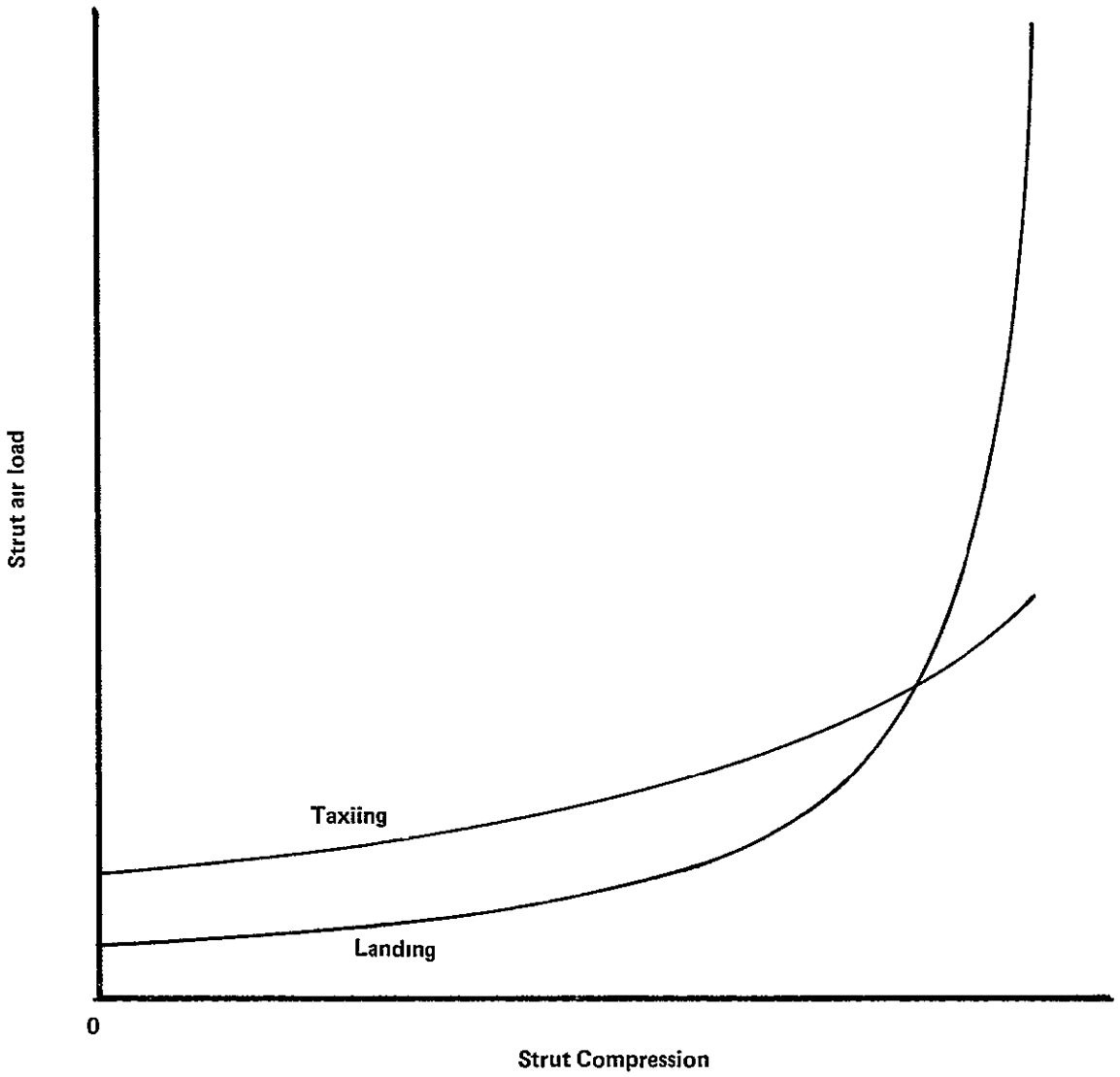

Figure 1. - Dual-mode adaptive landing gear system air curves.

TEST PROGRAM

Test Procedure

In order to determine the effectiveness of a softer air curve than normal, three series of test taxi runs were performed at Edwards AFB using the NASA YF-12A, S/N 935. The first series measured the airplane responses with the basic landing gear, the second and third series measured the responses with different configurations of soft gears. Figures 2 and 3 show the actual air curves tested for the three test series, for both the main and nose gears. Table 1 presents the volumes of the external air bottles and the fully extended strut inflation pressures.

During the second series of tests, a tendency for the nose gear to bottom in extension during taxiing, and possibly in compression during braking, was observed. From Figure 3, it can be seen that the fully extended nose gear load is only slightly below the static load range during the tests so that some bottoming in extension could be expected. Due to these problems, it was decided to employ a less flat air curve for the third series of tests. The main gears indicated no problems in this regard, so for the third series of tests the fully extended pressure was increased further to provide what is considered to be about as flat an air curve as practical for the static load range tested.

It should be noted that the DMS as defined in Reference 1 does not provide for altering the air curve in response to static load variations. A more elaborate system could be designed to tune the air curve to the current airplane weight and cg position. By this means an even flatter air curve could be employed than those used in the current study, since the range of static loads to be accommodated by a given air curve could be reduced to zero. Therefore, the present investigation is not to be viewed as the ultimate application of the adaptive gear concept, but as a test of the effect of certain specific variations in landing gear stiffness.

TABLE 1. - GEAR TEST PARAMETERS

Configuration	Main Gear		Nose Gear	
	Added Air Volume (in^3)	Inflation Pressure (psig)	Added Air Volume (in^3)	Inflation Pressure (psig)
I	0	280	0	245
II	300	560	100	410
III	300	678	50	325

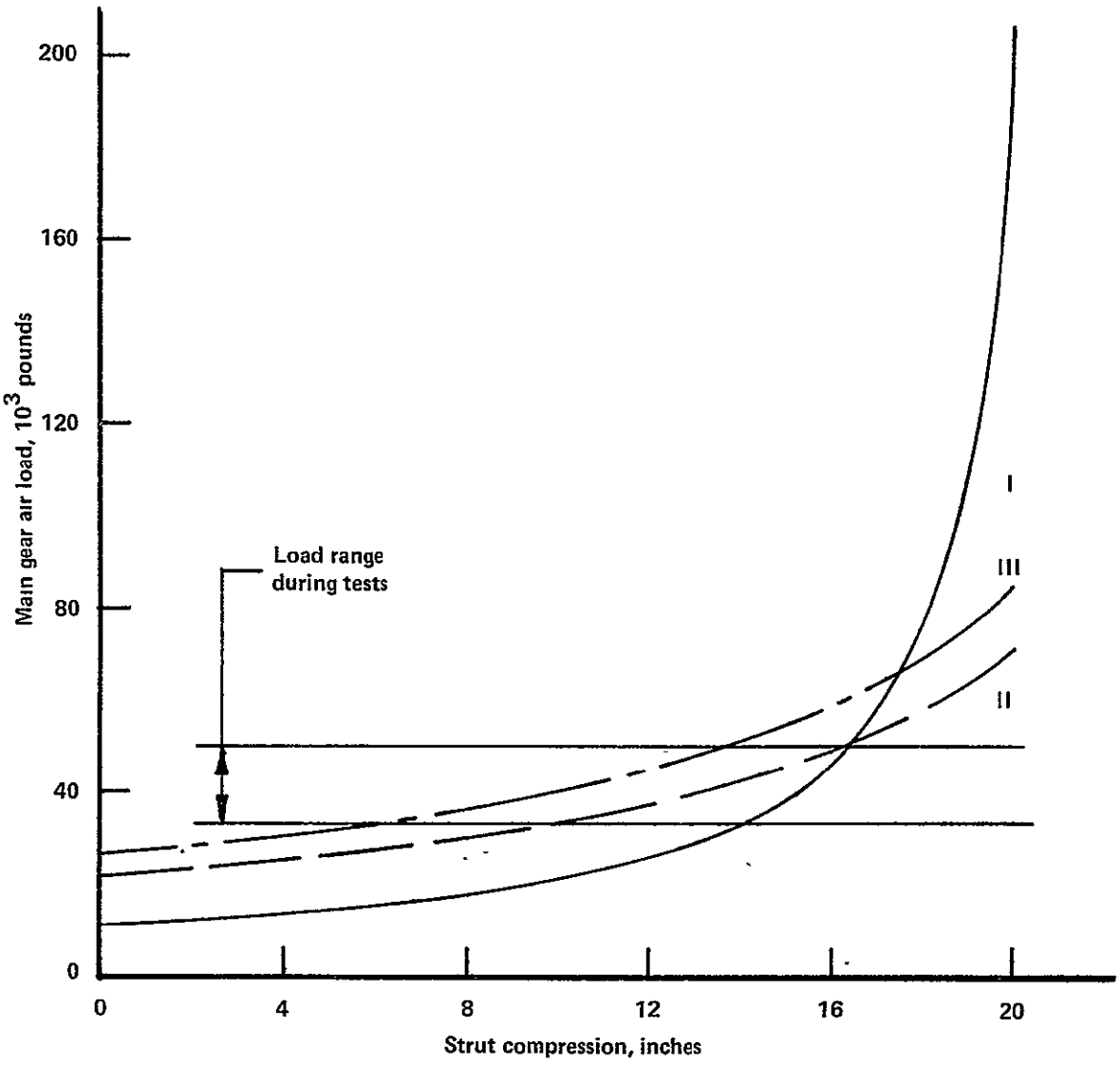

Figure 2. - Main gear test air curves.

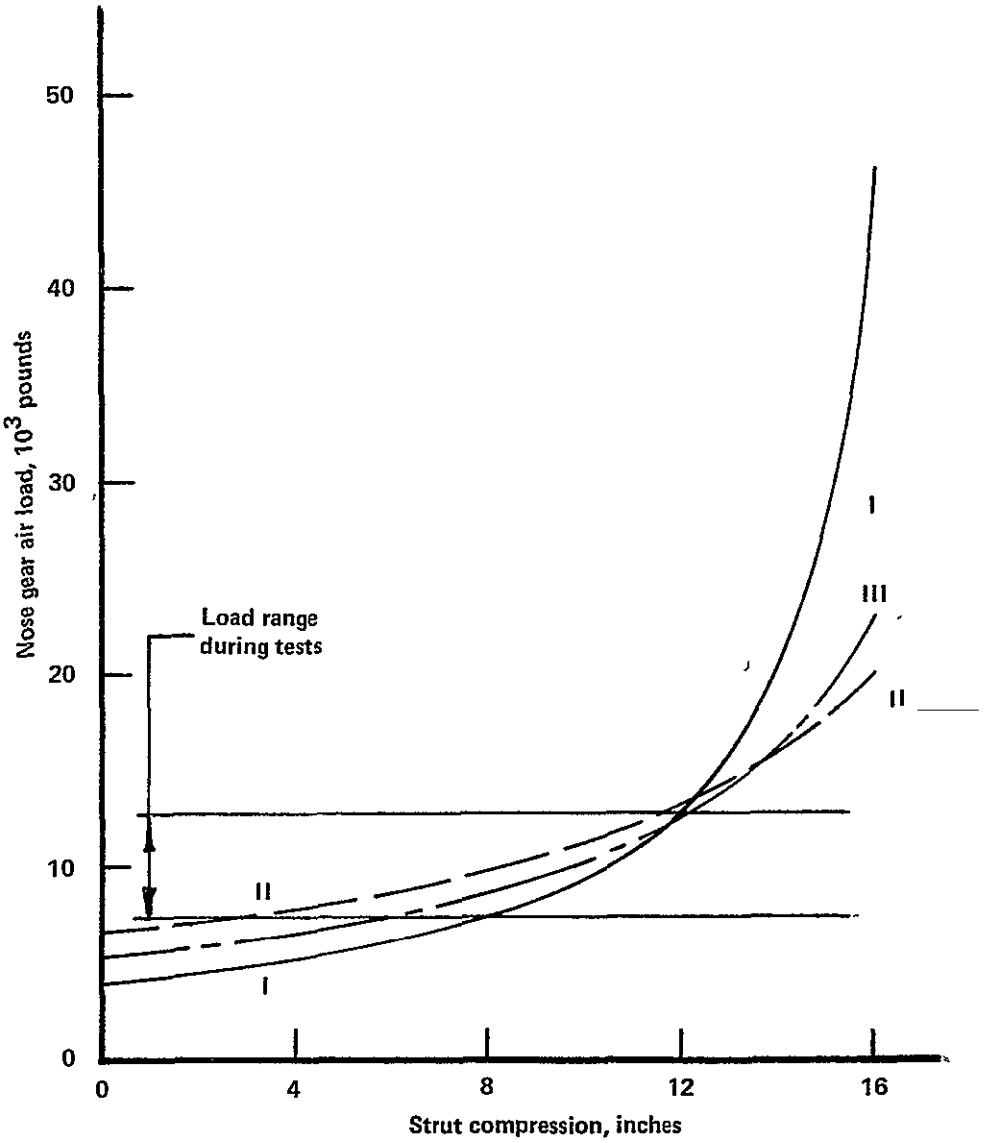

Figure 3. – Nose gear test air curves.

For each of the three landing gear configurations tested, a series of eight separate taxi runs was performed. Table 2 defines the testing sequence employed for each configuration.

Tire-cooling requirements necessitated a 10 to 15-minute cooling period using fans between runs. After Run 5, a 1-hour cooling period, with fans, was required. Runs 1 and 2 consisted of acceleration to test speed, maintaining a constant test speed for 10 to 12 seconds, and braking to taxi speed at the opposite end of the runway. Runs 3 and 6 followed the same pattern, except that after the constant-velocity test run, the airplane accelerated to takeoff. Run 4 was a touch and go with a constant-speed taxi period while on the ground. Runs 5 and 7 were landings involving heavy braking to the test speed, a constant-velocity period of 10 seconds, followed by chute deployment and braking to a stop. Run 8 was the same as 1 and 2 except for taxiing back to NASA.

This entire set of 8 runs took approximately 4 hours to perform. The tests were run on 2/28/78, 3/7/78 and 3/15/78. The purpose of the test procedure outlined in Table 2 was to provide constant-speed taxi test data at a range of airplane weights and velocities. For each of the three series of runs, the attempt was made to duplicate the airplane weight, cg position, velocity, and position on the runway so that direct comparisons could be

TABLE 2. - TEST RUN CONDITIONS

Test Run	Runway	Weight (Pounds)	CG (% MAC)	Speed (Knots)
1	04	108 000	19.9	75
2	22	105 000	20.05	90
3	04	101 000	19.8	105
	(Continue to takeoff - burn down to 94 000 - 20.4%)			
4	Land 22	94 000	20.4	155
	(Continue to takeoff - burn down to 90 000 - 20.6%)			
5	Land 22	90 000	20.6	120
	(Burn 8000 at idle or defuel/shut down engines - cool brakes and tires one hour - reload drag chute)			
6	04	82 000	20.7	105
	(Continue to takeoff - burn down to 76 000 - 20.8%)			
7	Land 22	76 000	20.8	90
8	04	73 000	19.9	70
	END TEST			

made of the effects of different gear air curves. Although actual landings were made as part of the test procedure, the air curves were always fixed to one of the three curves shown in Figures 2 and 3. Therefore, for the second and third series of tests, the airplane was actually landed on the flat air curves designed for taxiing. Data for the airplane responses during these landing impacts was not processed; only the constant-velocity taxi data was examined.

Test Results

While the test procedure called for taxiing at constant velocity over the same section of runway for each of the three series of tests for a given run, in practice the airplane traversed somewhat different sections of runway from one test series to the next. Figure 4 illustrates the actual portion of the runway covered for each of the 8 runs for the three test series. The Roman numerals on the bar graphs identify the end points of the constant-velocity portion of each run; I represents the first series, II the second series and III the third series.

The position of the airplane on the runway is determined by a theodolite optical triangulation system which is called ASKANIA. For Runs 1, 5, and 6 of Test Series I, this system failed to function, so the position of the airplane on the runway is unknown for these three runs. Therefore, these runs cannot be used for comparison of results with different air curves. For the remaining runs, Table 3 shows the average velocity and the portion of the runway common to all three test series. Also shown is the difference between the maximum and minimum velocity for each run. Runs 7 and 8 exhibit the greatest velocity variation, representing about 6 percent. The five runs shown in Table 3 constitute about 42 seconds for each test series of runs performed at about the same velocity and on the same section of runway.

Table 4 summarizes the actual test airplane weight and cg position for the five usable runs. The largest deviation in test weight from Series I to Series III occurred for Run 8, and the difference of 2100 pounds represents less than a 3 percent variation.

Accelerometer time history traces from the three sets of five runs are processed in the following fashion. For each response quantity, a cumulative frequency of exceedance (peak count) curve is developed for each run for each test series. For a given series, these peak counts are added for all five runs, representing a 42-second exposure at various airplane weights and velocities. These cumulative exposure exceedance curves are then compared for the three test series to examine the effect of varying the landing gear air curve. Each peak in a peak count of a time history is defined as the maximum or minimum value attained between zero-level crossings.

The method described is used to provide a statistically more complete description of the characteristics of the time histories than is obtained

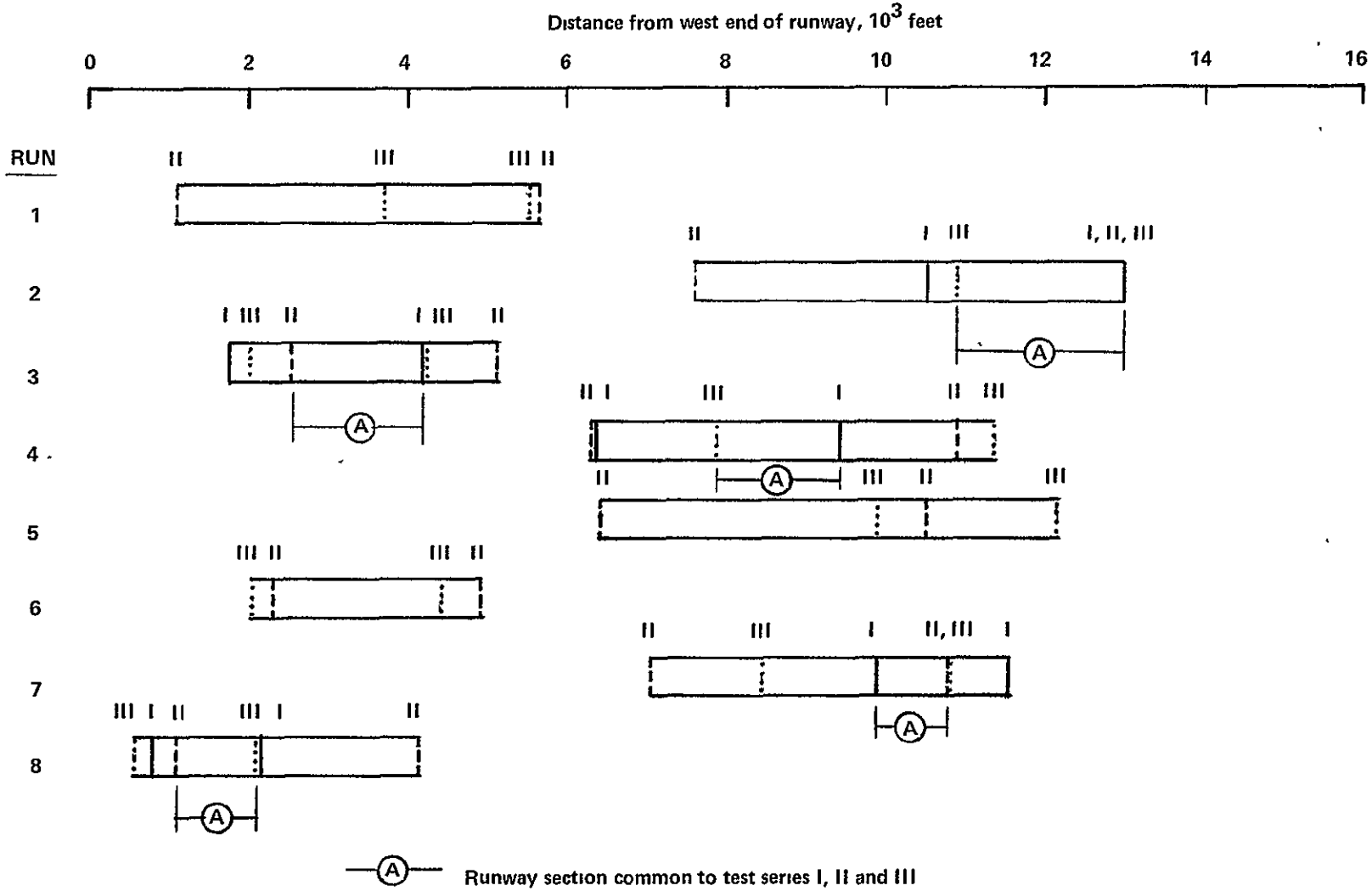

Figure 4. - Airplane position on runway during tests.

TABLE 3. - POSITION AND VELOCITY TEST PARAMETERS

Run	① Position (feet)	Average Velocity (knots)			Velocity Range (knots)
		I	II	III	
2	12890 - 10900	94.5	91.9	92.3	2.6
3	2540 - 4180	111.4	110.5	107.1	4.3
4	9470 - 7870	153.5	157.6	156.1	4.1
7	10770 - 9840	89.7	95.6	92.1	5.9
8	1110 - 2130	76.9	72.5	72.2	4.7

① Initial and final positions, as measured from west end of runway

TABLE 4. - AIRPLANE WEIGHT AND CG TEST PARAMETERS

Run	Weight, 10^3 Pounds			CG Position, % MAC		
	I	II	III	I	II	III
2	105.3	106.0	106.3	20.3	20.0	20.2
3	102.7	103.0	101.7	20.2	19.3	19.9
4	93.0	94.7	94.6	20.0	20.0	19.9
7	76.0	74.2	74.0	20.0	20.0	20.2
8	73.0	71.0	70.9	19.6	19.4	19.9

by merely tabulating the maximum single peaks observed for each run. Although the mix of airplane weights and velocities used is not necessarily representative of any specific airplane mission or operation, the weights and velocities encompass a broad range of actual operational conditions. In other words, the exceedance curves derived from adding the five runs for each configuration are not necessarily an accurate estimate of a typical ground taxi load spectrum, but rather represent the summation of the available comparative test data encompassing realistic operational weights and velocities.

Figures 5 through 9 show comparisons of exceedance curves for normal (vertical) acceleration measured at five locations on the test airplane. Table 5 defines the specific locations of the five accelerometers, while Figure 10 shows their location on a plan view of the airplane. Figures 5 and 6 indicate that significant reductions occur in the cg and cockpit

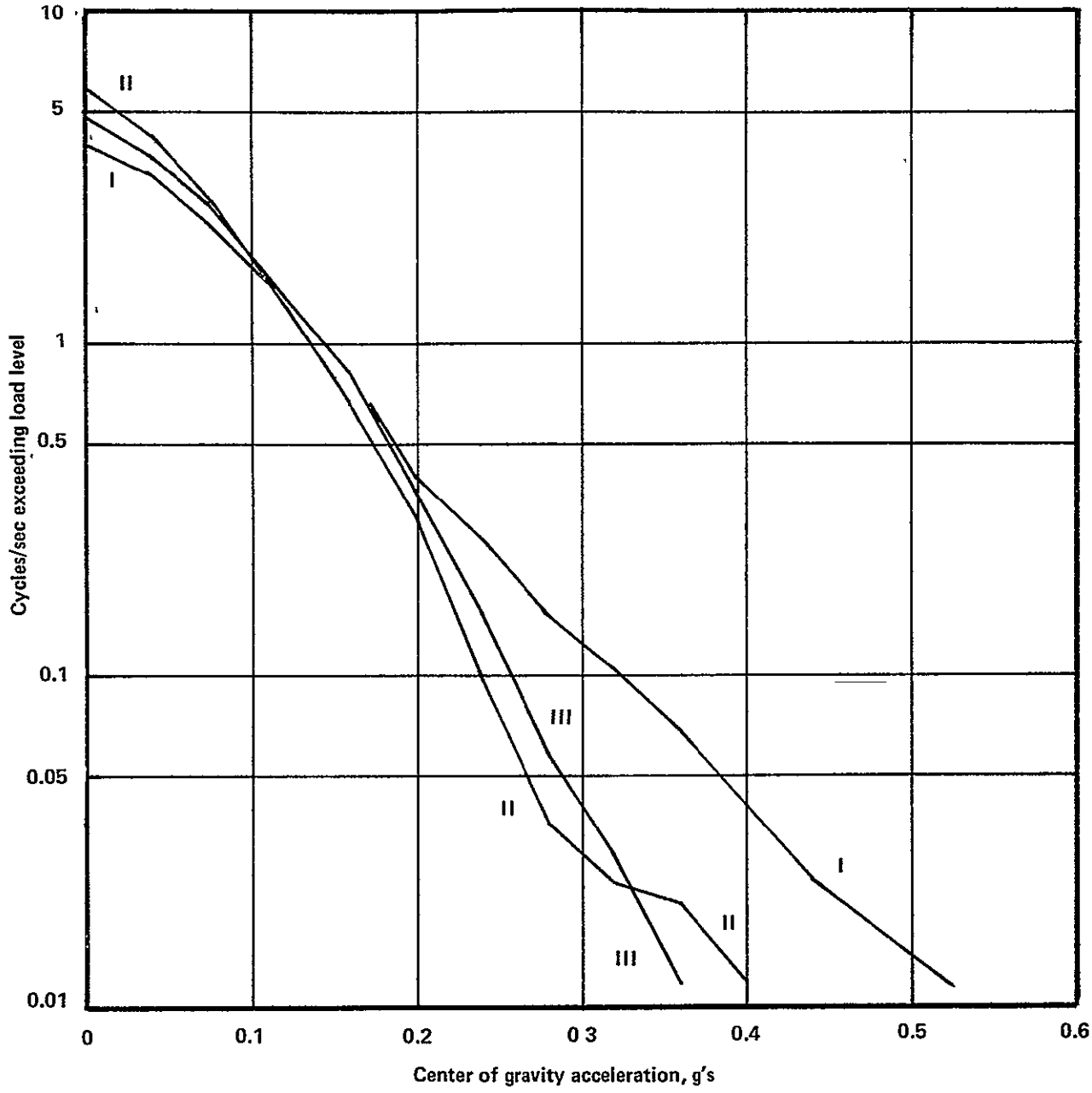

Figure 5. - Test exceedance curves, cg acceleration.

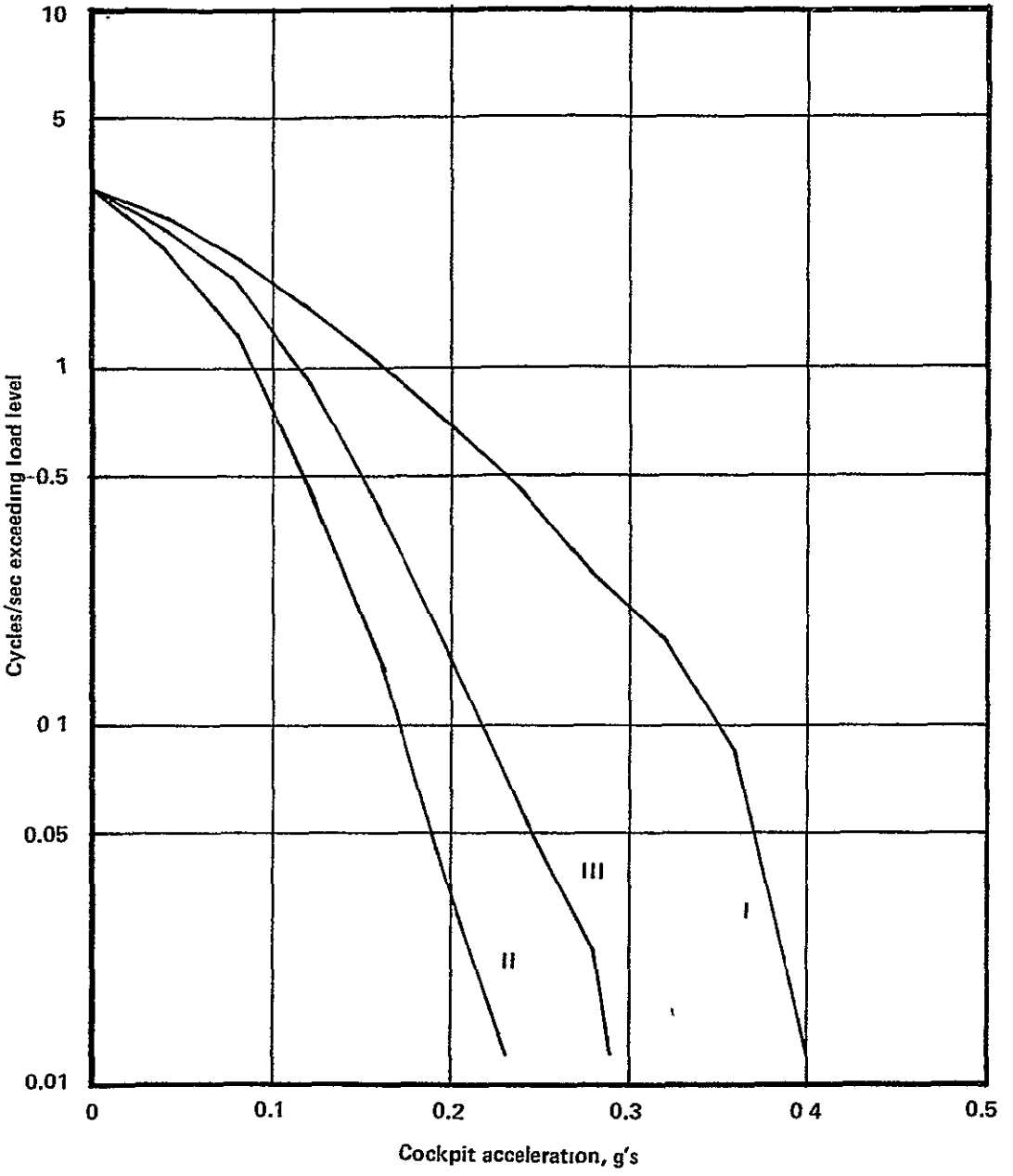

Figure 6. - Test exceedance curves, cockpit acceleration.

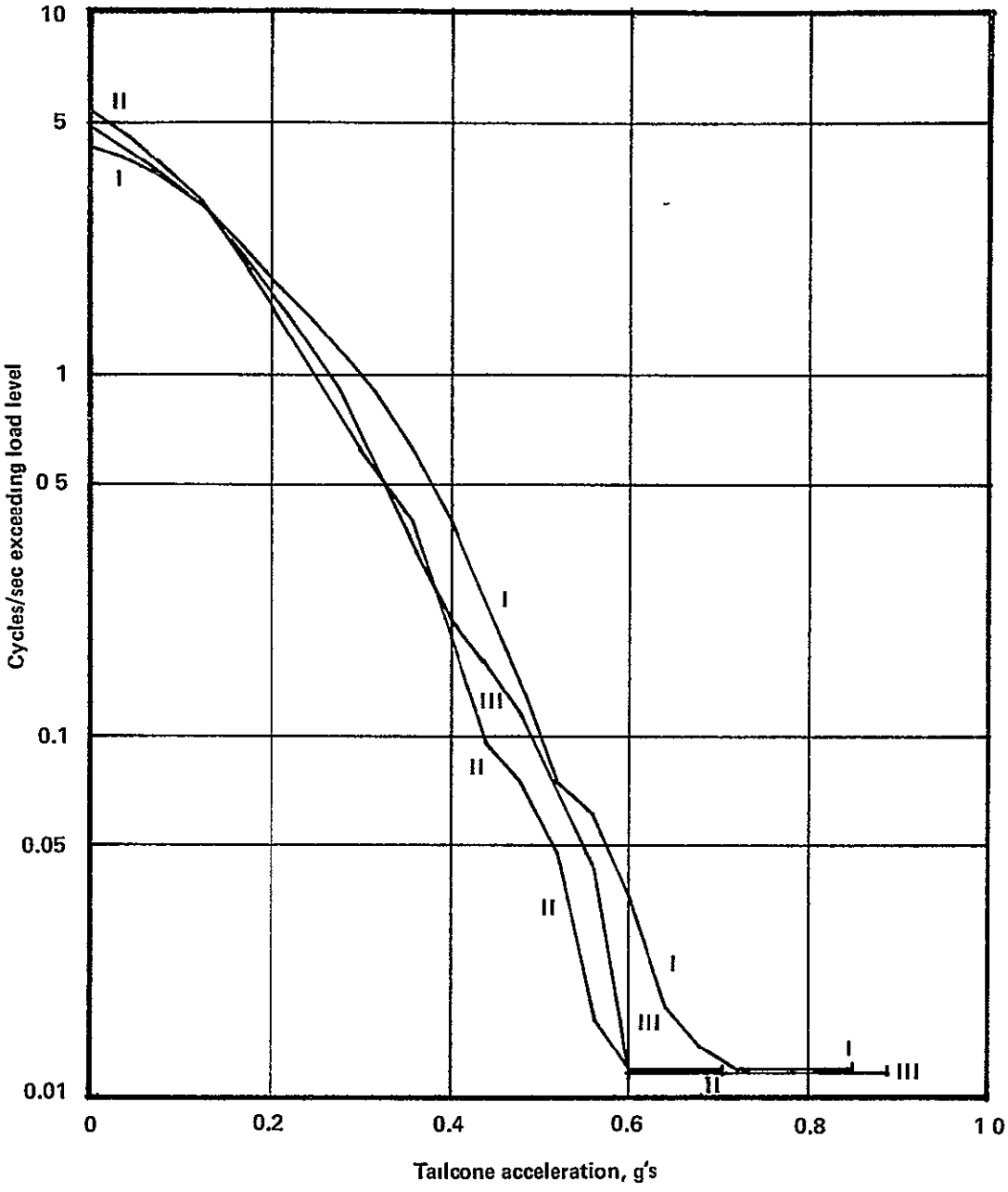

Figure 7. - Test exceedance curves, tailcone acceleration.

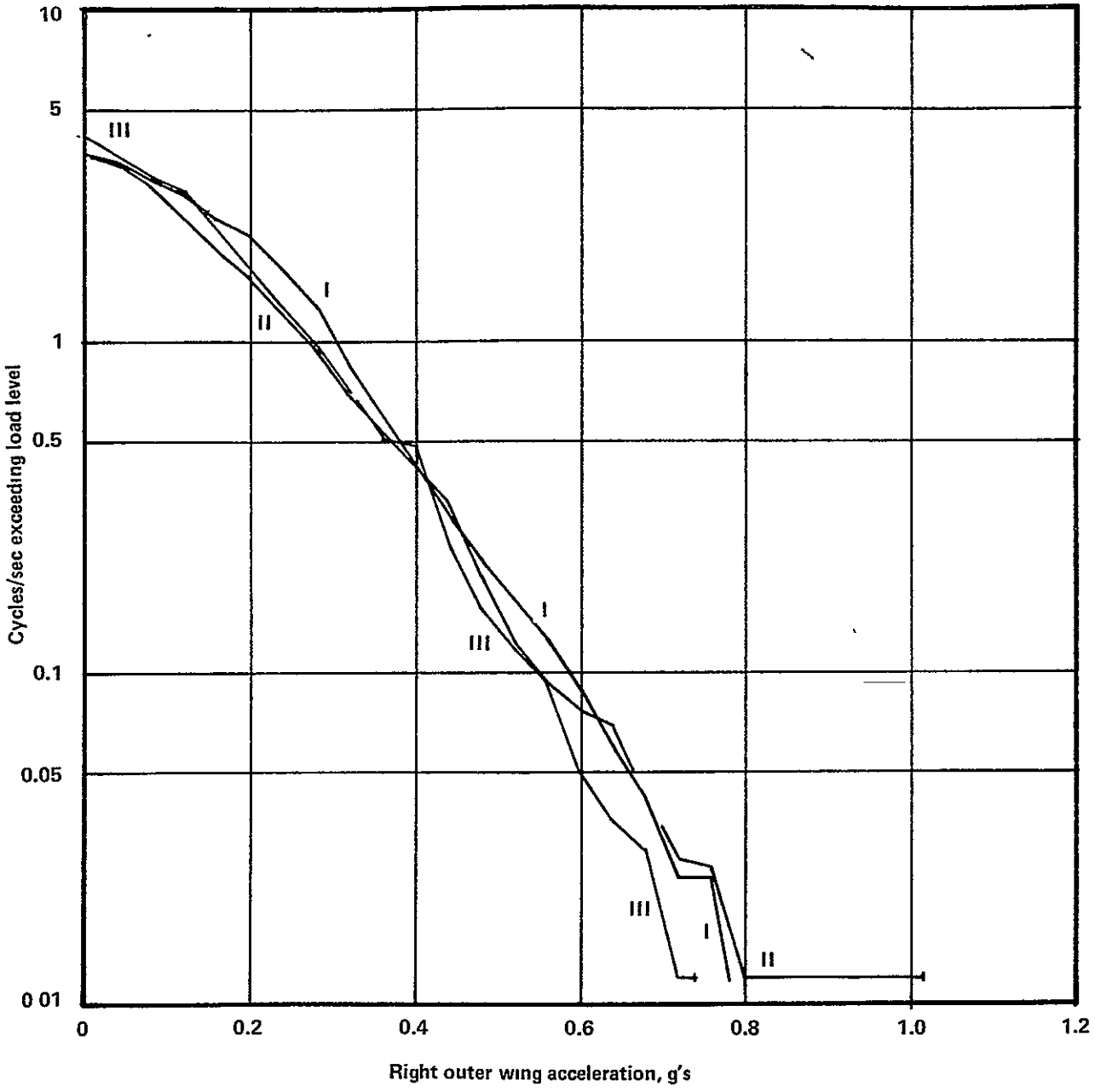

FIgure 8. - Test exceedance curves, right outer wing acceleration.

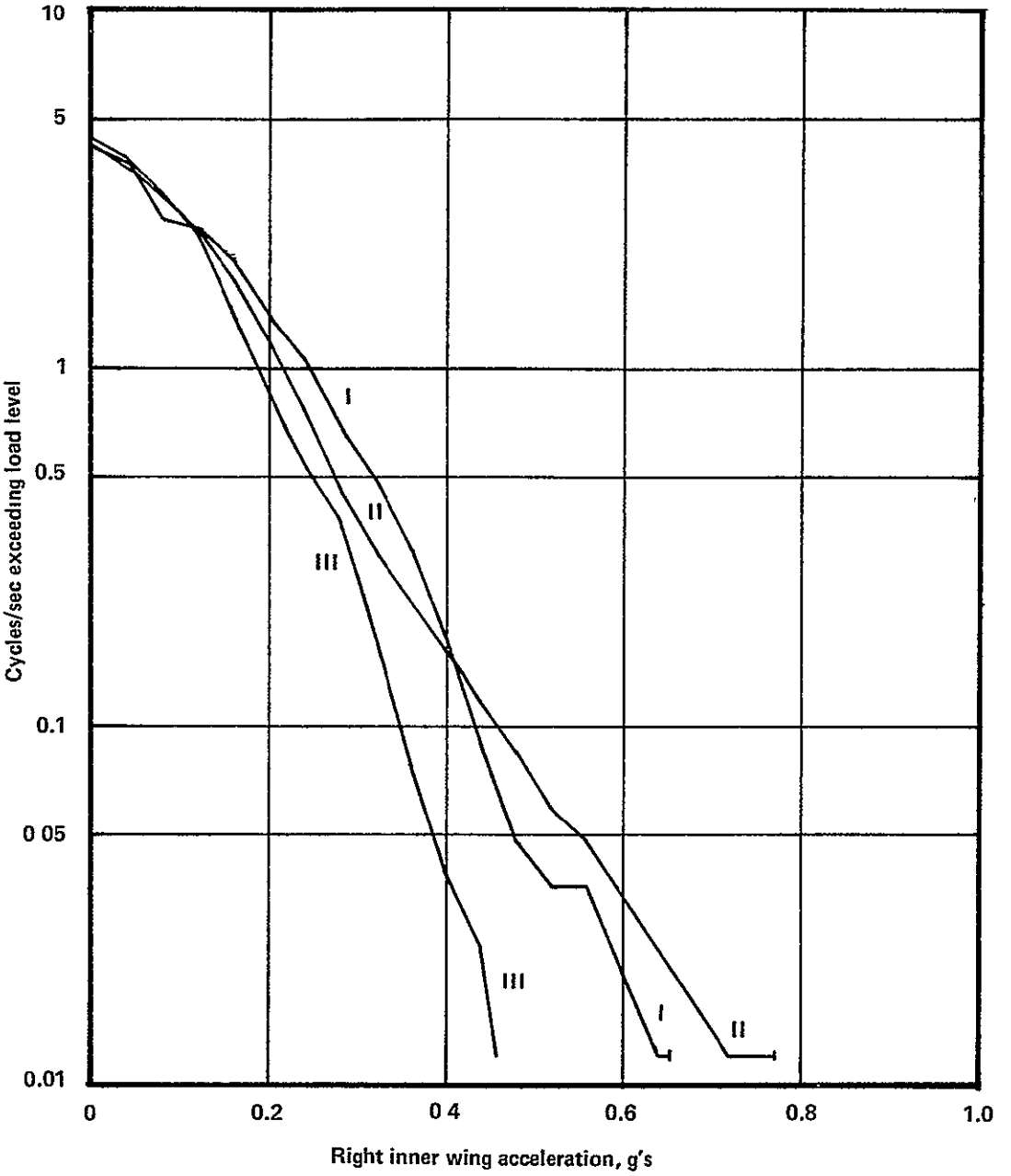

Figure 9. - Test exceedance curves, right inner wing acceleration.

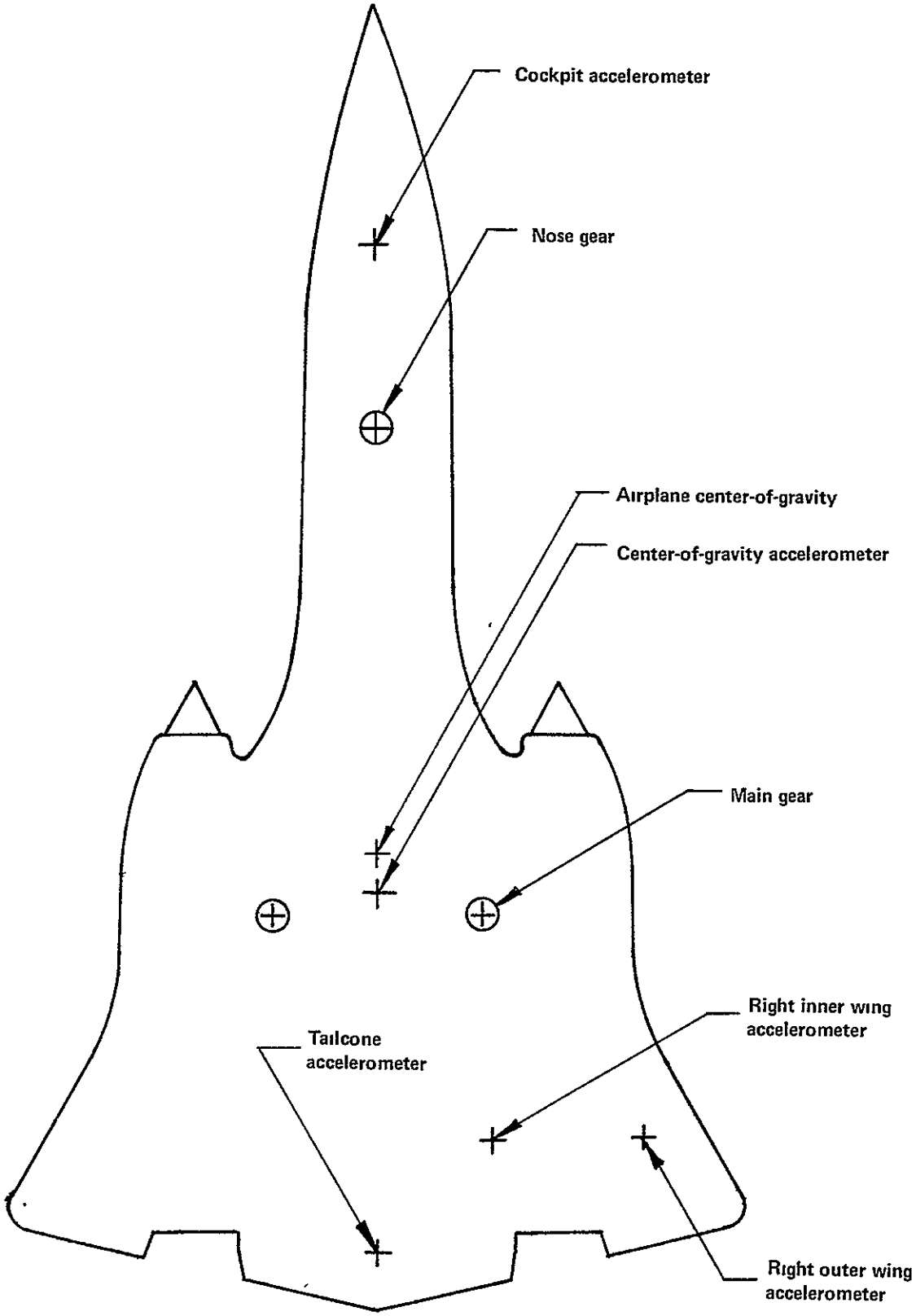

Figure 10. - Accelerometer locations.

TABLE 5. - TEST AIRPLANE ACCELEROMETER LOCATIONS

Description	Accelerometer Designation	FS	BL
Center of Gravity	A 4001	915	0
Cockpit	A 4004	310	0
Tailcone	A 4030	1258.9	1.56 right
Right Outer Wing	A 4033	1135.4	247.5
Right Inner Wing	A 4034	1140.2	106.9

acceleration response levels for both configurations of reduced-stiffness air curves. The cg acceleration levels are reduced in the order of 25 percent for either Configuration II or III, while the cockpit acceleration levels are reduced by 30 percent for Configuration III and 45 percent for Configuration II. The superior performance of Configuration II compared to III for cockpit accelerations is attributed to the softer nose gear air curve for Configuration II compared to III, as seen in Figure 3.

Figures 7, 8 and 9 show exceedance curves for the accelerations at three locations in the aft end of the airplane. These curves do not indicate the clear response level reductions evident in Figures 5 and 6. For the tailcone, reductions in the order of 10 to 15 percent are achieved if the single discrete peaks are ignored. (The single largest peak shows up as a horizontal line at the bottom of the exceedance curve.) For the right outer wing, Configuration II is about the same as the basic gear, while Configuration III shows about a 6-percent reduction compared to the basic gear. The right inner wing shows a clear reduction for Configuration III of about 20 to 30 percent, while Configuration II is about 15 percent worse than the basic gear.

After the second series of tests, the pilot commented that the ride felt rougher than the basic airplane. However, this was a different pilot than the one who flew the first series of tests, so his comparisons are based on general YF-12 operations at Edwards AFB, rather than direct comparison between Test Series I and II. An examination of Figure 6, showing cockpit acceleration levels reduced substantially for Test Series II, does not correlate with the pilot's comments. The pilot for Test Series III was the same as for Series I, and he commented that the Series III ride was smoother than the Series I, particularly at the high gross weights.

However, for Series III, the pilot felt that there was considerable hammering of the main gears during rotation to takeoff for Runs 3 and 6. He commented that this effect was significant enough to cause the pilot to hurry the rotation. Examination of the time history traces for the rotation

portion of Runs 3 and 6 shows no unusual responses for the main or nose gears, except that during Run 6 the nose gear, upon going fully extended, cycles back into compression twice over a period of 2 seconds before staying fully extended. It is possible that the pilot felt a hard extension of the nose gear, but that doesn't show up as anything significant in the gear-force time histories. Landing gear bottoming in compression could be prevented by the inclusion of snubbers that are effective only near bottoming.

The pilots occasionally complained of hard landings during the second and third series of tests. This is to be expected, since the airplane was being landed on air curves having considerably increased fully extended gear loads (breakout loads). In a complete dual-mode system, landings would always be performed with the normal air curve.

ANALYTICAL PROGRAM

Single-Degree-of-Freedom Analysis

In order to obtain a first order estimate of the magnitude of the reduction in dynamic response attainable with a reduced stiffness air curve, a linear single-degree-of-freedom (SDOF) spring-mass-damper system is examined. This system is intended to represent a single main landing gear, with the mass corresponding to the static load on the gear. The acceleration response of this mass is a rough measure of the airplane cg acceleration response. The runway is modeled as a random displacement input having a Power Spectral Density (PSD) given by Equation (1).

$$\phi(\Omega) = C\Omega^{-2} \tag{1}$$

where

$\phi(\Omega)$ = Power Spectral Density, $ft^2/rad/ft$

C = Constant defining level of runway roughness

Ω = Reduced frequency, rad/ft

The reduced frequency is defined as

$$\Omega \triangleq \omega/V \tag{2}$$

where

ω = Angular frequency, rad/sec

V = Airplane velocity, ft/sec

The general form of Equation (1) is commonly used to represent runway roughness. Reference 2 indicates that the exponent varies from one runway to another, but the value generally lies in the range of 1.9 to 2.1.

For a linear SDOF system, the transfer function relating mass acceleration output to displacement input at the spring-damper is given by Equation (3).

$$T(\omega) = \alpha^2 \omega_n^2 \left[\frac{1 + 4\zeta^2 \alpha^2}{(1 - \alpha^2)^2 + 4\zeta^2 \alpha^2} \right]^{1/2} \quad (3)$$

where

$\alpha = \omega / \omega_n$

ω = Angular frequency, rad/sec

ω_n = Natural frequency, rad/sec

ζ = Damping ratio (Actual damping/critical damping)

The general expression for the root-mean-square (rms) response of a linear system to a random input with a specified PSD is given by

$$\sigma = \left\{ \int_0^\infty \phi(\omega) \left| T(\omega) \right|^2 d\omega \right\}^{1/2} \quad (4)$$

Combining Equations (1) through (4) results in the following expression for the rms acceleration of a linear SDOF system subjected to random runway roughness input.

$$\sigma = \sqrt{CV}\, \omega_n^{3/2} \overline{\sigma} \quad (5)$$

where

$$\overline{\sigma} = \left\{ \int_0^\infty \alpha^2 \left[\frac{1 + 4\alpha^2 \zeta^2}{(1 - \alpha^2)^2 + 4\alpha^2 \zeta^2} \right] d\alpha \right\}^{1/2} \quad (6)$$

Equation (5) indicates that the rms acceleration is proportional to the square root of airplane velocity, the 1.5 power of the natural frequency, and is a function of the damping ratio ζ. Figure 11 is a plot of $\overline{\sigma}$ versus damping ratio from Equation (6), using finite integration limits of $\alpha = 0.1$ to $\alpha = 10$. Notice that Figure 11 implies that there is an optimum damping ratio on the order of $\zeta = 0.22$.

Appendix E of Reference 2 describes procedures for determining an equivalent linearzation for a nonlinear landing gear. Applying these techniques

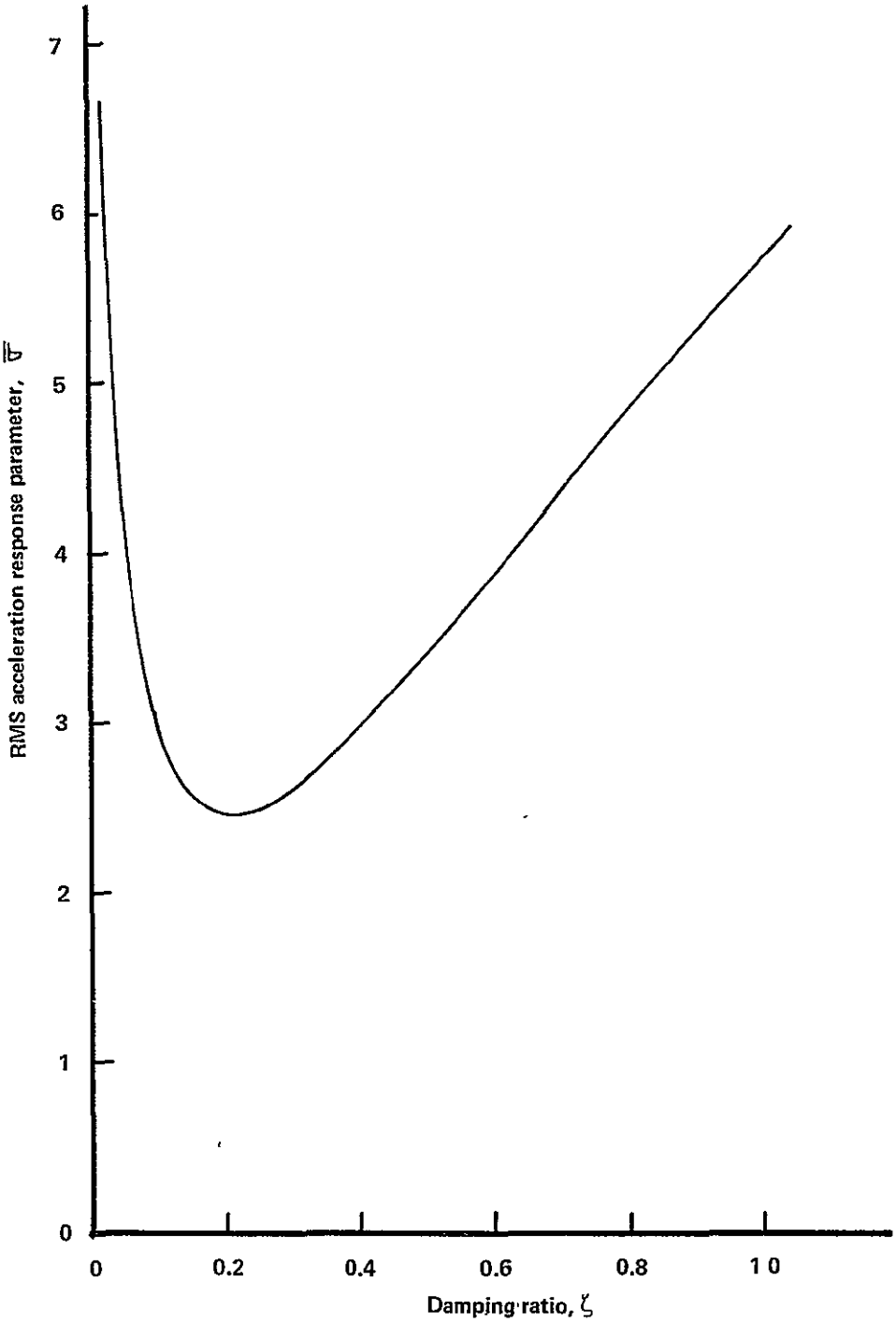

Figure 11. - RMS acceleration response parameter.

to the YF-12A test airplane, and using Equation (5) and Figure 11, the relative cg acceleration responses shown in Table 6 are obtained.

Note that as the main gear stiffness is reduced, the damping ratio increases because the actual damping constant is not changed. From Figure 11, for damping ratios greater than the optimum value, an increase in ζ results in an increase in the factor $\overline{\sigma}$. This increase tends to reduce the direct benefits of the $\omega_n^{3/2}$ term in Equation (5). (ω_n reduces as the square root of the gear stiffness reduction.) The final column in Table 6 shows the predicted reduction in cg rms acceleration levels for Test Series II and III, relative to Series I. For this comparison, the factor $\sqrt{CV}$ in Equation (5) is not evaluated, since the runway exposure and airplane velocities are the same for all three test series.

Figure 12 shows the σ/σ_I from Table 6, plotted against the gear natural frequency. The right-hand data point represents the conditions for Test Series I. The top two curves are test data taken from Figure 5, using the single peak value and the response level at a frequency of 0.1 cycles per second. The solid line represents the predicted results from Equation (5) and Table 6. Also shown is the predicted relative response if the damping ratio were held constant by varying the orifice damping characteristic as the gear stiffness is changed. Significantly improved performance is predicted using this technique. The bottom line in Figure 12 shows the relative responses that would be achieved if the responses were directly proportional to the equivalent linear gear stiffness. Although Equation (5) does not predict this relationship, certain simplified dynamic taxi load prediction methods are based on this assumption. Figure 12 shows that Equation (5) represents a fairly accurate estimate of the observed test data, and that the bottom line is overly optimistic.

The results shown in Figure 12 indicate that the test data are in good agreement with the anticipated results based on simple SDOF linear model considerations. It should be noted that the responses at other locations on the airplane cannot be predicted with this simple scheme, and that the apparent inconsistencies in Figures 7 through 9 could never be analytically predicted by Equation (5), or by any single-degree-of-freedom analysis.

TABLE 6. - PREDICTED RELATIVE RESPONSES, SINGLE-DEGREE-OF-FREEDOM SYSTEM

Test Series	Main Gear Stiffness (#/in.)	Damping Ratio (ζ)	Natural Frequency (Hz)	$\omega_n^{3/2}$	$\overline{\sigma}$	$\omega_n^{3/2}\overline{\sigma}$	σ/σ_I
I	6237	0.355	1.217	1.343	2.80	3.759	1.000
II	2560	0.555	0.779	0.688	3.68	2.530	0.674
III	2143	0.606	0.713	0.602	3.91	2.354	0.627

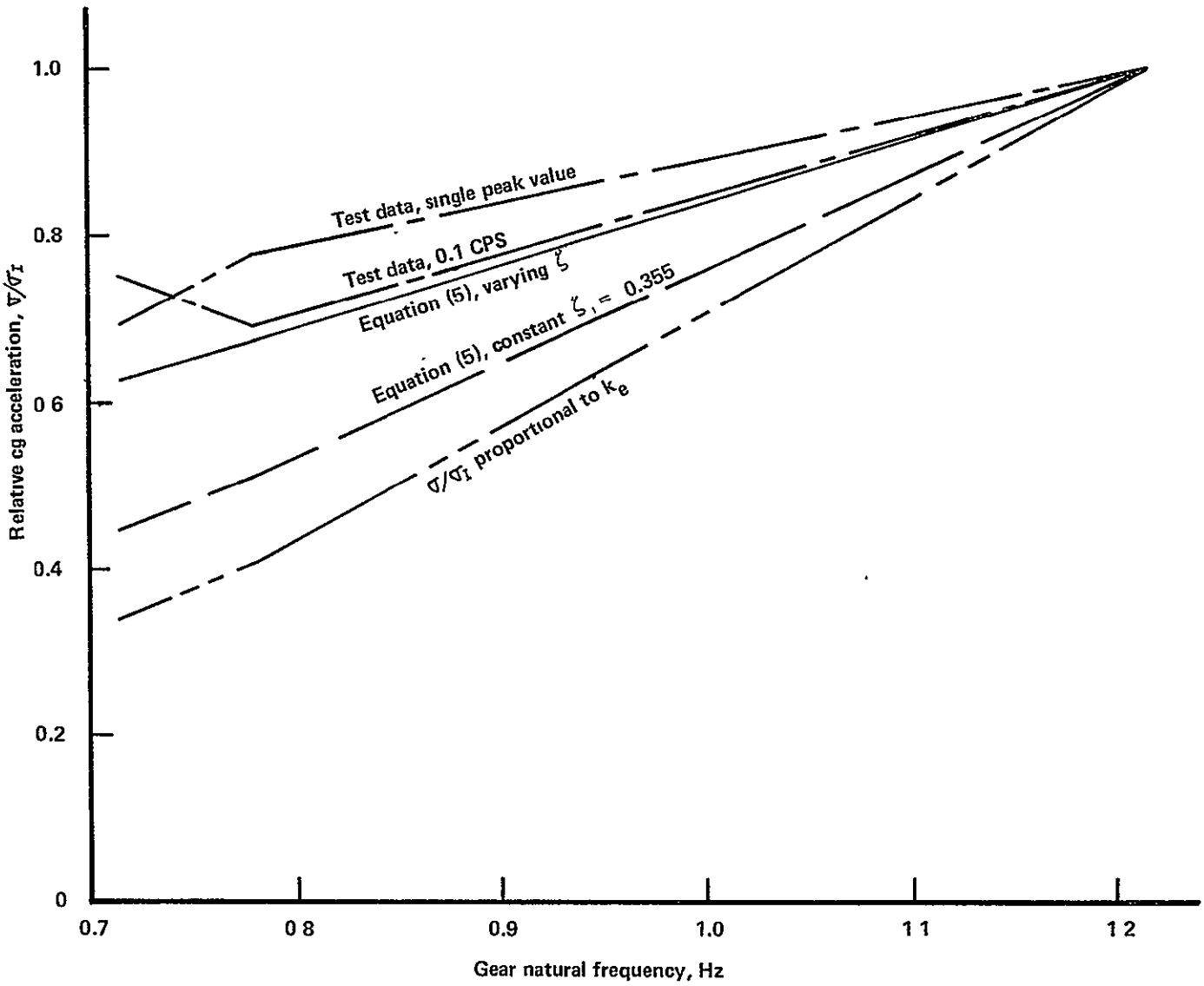

Figure 12. - Relative cg acceleration, test versus theory.

Dynamic Taxi Computer Program Analysis

Analyses of the dynamic taxi responses of the YF-12A were made using a digital computer program described in Reference 3. The Edwards AFB runway profile as surveyed by NASA was used as input to the program. Since the pilots deliberately lined up the nose gear about 6 to 10 feet south of the runway centerline, the following profile tracks are used in the analysis:

Right Main Gear - 18 feet right of centerline

Left Main Gear - Centerline

Nose Gear - 6.25 feet right of centerline

The preceding pattern is used for all runs heading east; for runs heading west, the right and left main gear inputs are reversed.

The computer program models the airplane's pitch, plunge, and roll rigid body degrees-of-freedom, with the vehicle's flexibility represented by normal modes of vibration. The landing gears are modeled as conventional nonlinear pneumatic/hydraulic struts, with vertical degrees-of-freedom of the unsprung masses. Computer simulations were made to represent the test conditions shown in Table 3, with the airplane weight and cg positions defined in Table 4. Airplane normal modes of vibration were not generated specifically for each of the airplane weight conditions defined by Table 4. The modal data generated in support of the LAMS YF-12 Feasibility Study, NASA CR-2158, were used. These data are available only at weights of 124,271 pounds and 68,693 pounds, whereas the test weights for the current program range between 73,000 pounds and 105,300 pounds. Therefore, for Runs 2, 3, and 4 in Table 4, the mode shapes at 124,271 pounds are used, with the generalized masses reduced in proportion to the airplane weight. For Runs 7 and 8, the mode shapes at 68,693 pounds are used, with the generalized masses increased in proportion to the airplane weight. Furthermore, only symmetric modal data are used, since no antisymmetric modal data were generated for the LAMS Study.

Figures 13 through 22 show comparisons of analytical and test results for Test Series I and III, for the five accelerations for which the test data have been reduced. The analytical results shown in these figures use the first eight (lowest frequency) symmetric airplane normal modes. The cg acceleration comparisons shown in Figures 13 and 14 show excellent agreement between test and analytical results. The tailcone and right inner wing accelerations exhibit good correlation between test and analytical results, while the right outer wing acceleration correlation is poor and the analytical cockpit accelerations are substantially greater than the test results. The correlation at the right outer wing station would improve with the inclusion of anti-symmetric flexible modes, which were not available for this analysis. Further details concerning the correlation study are contained in Appendix A.

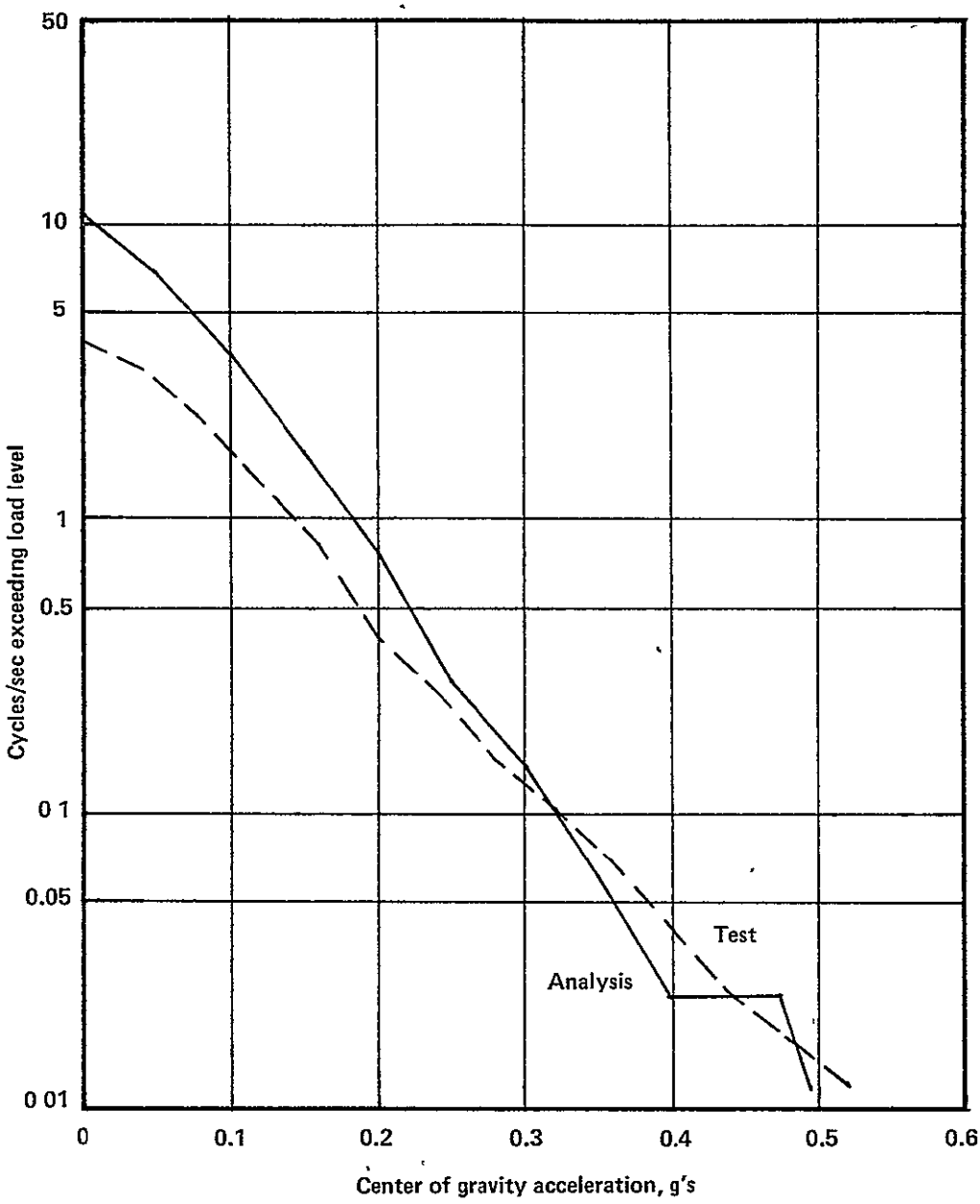

Figure 13.- Comparison of analytical and test results, cg acceleration, Test Series I

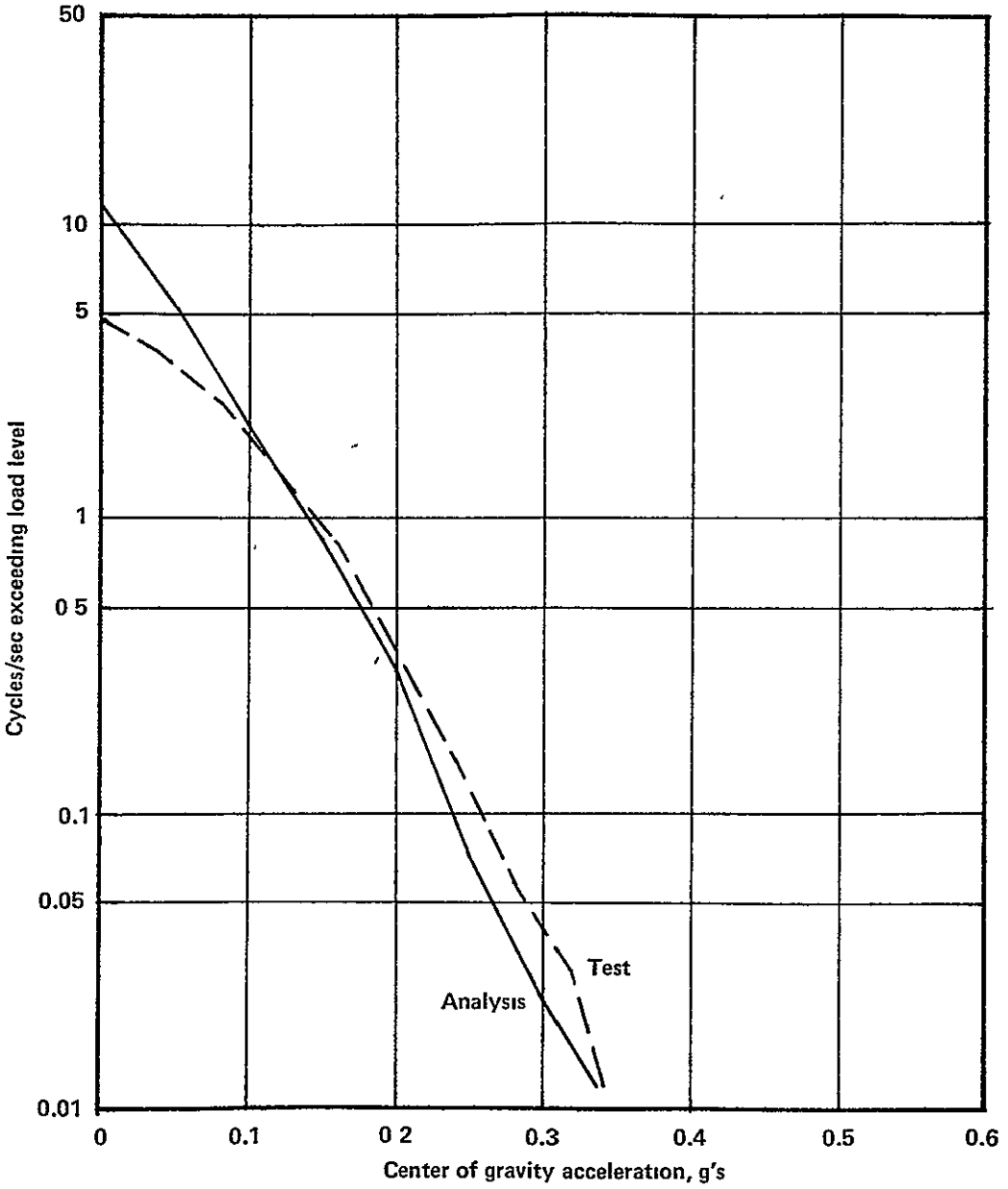

Figure 14.- Comparison of analytical and test results, cg acceleration, Test Series III.

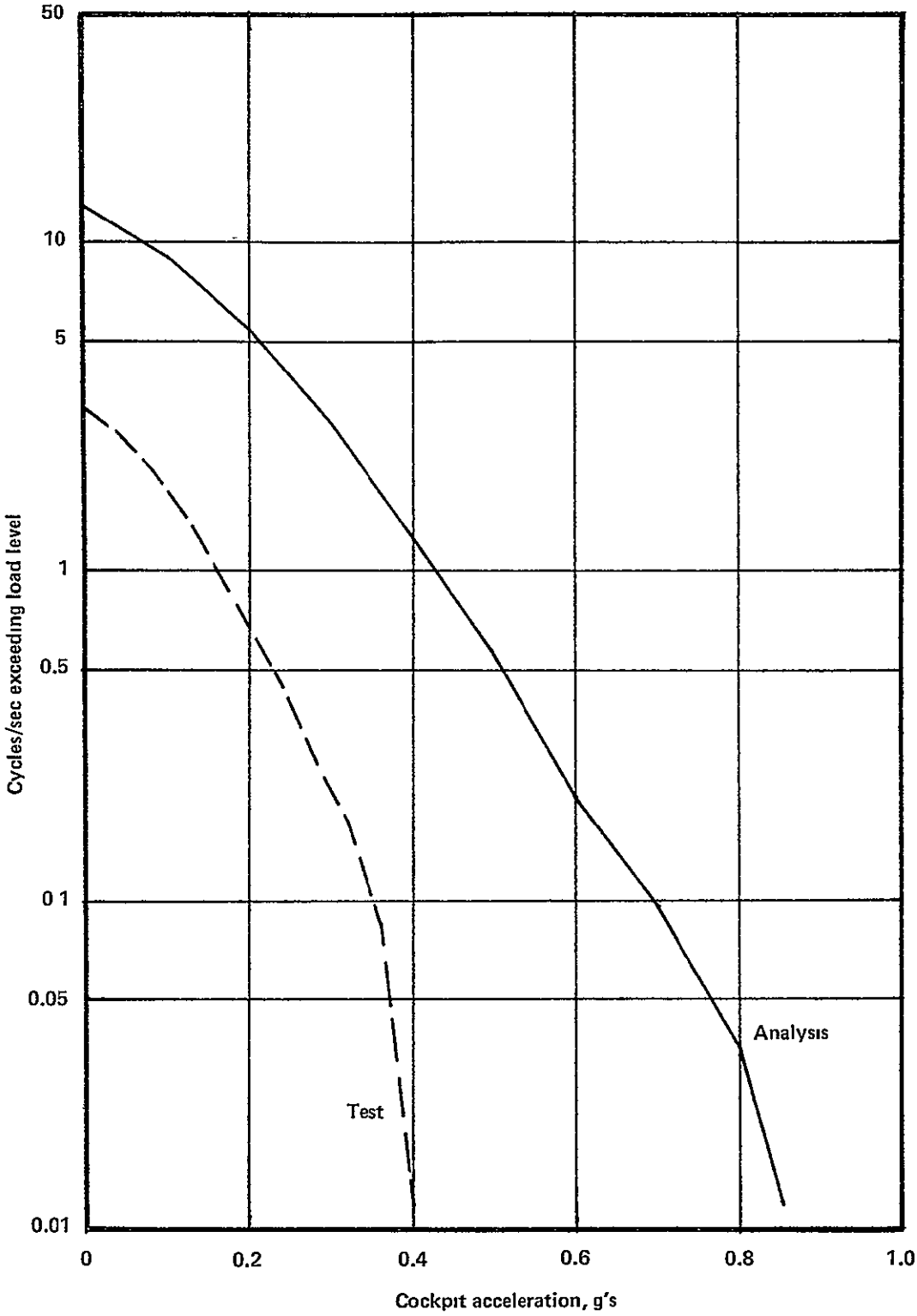

Figure 15.- Comparison of analytical and test results, cockpit acceleration, Test Series I.

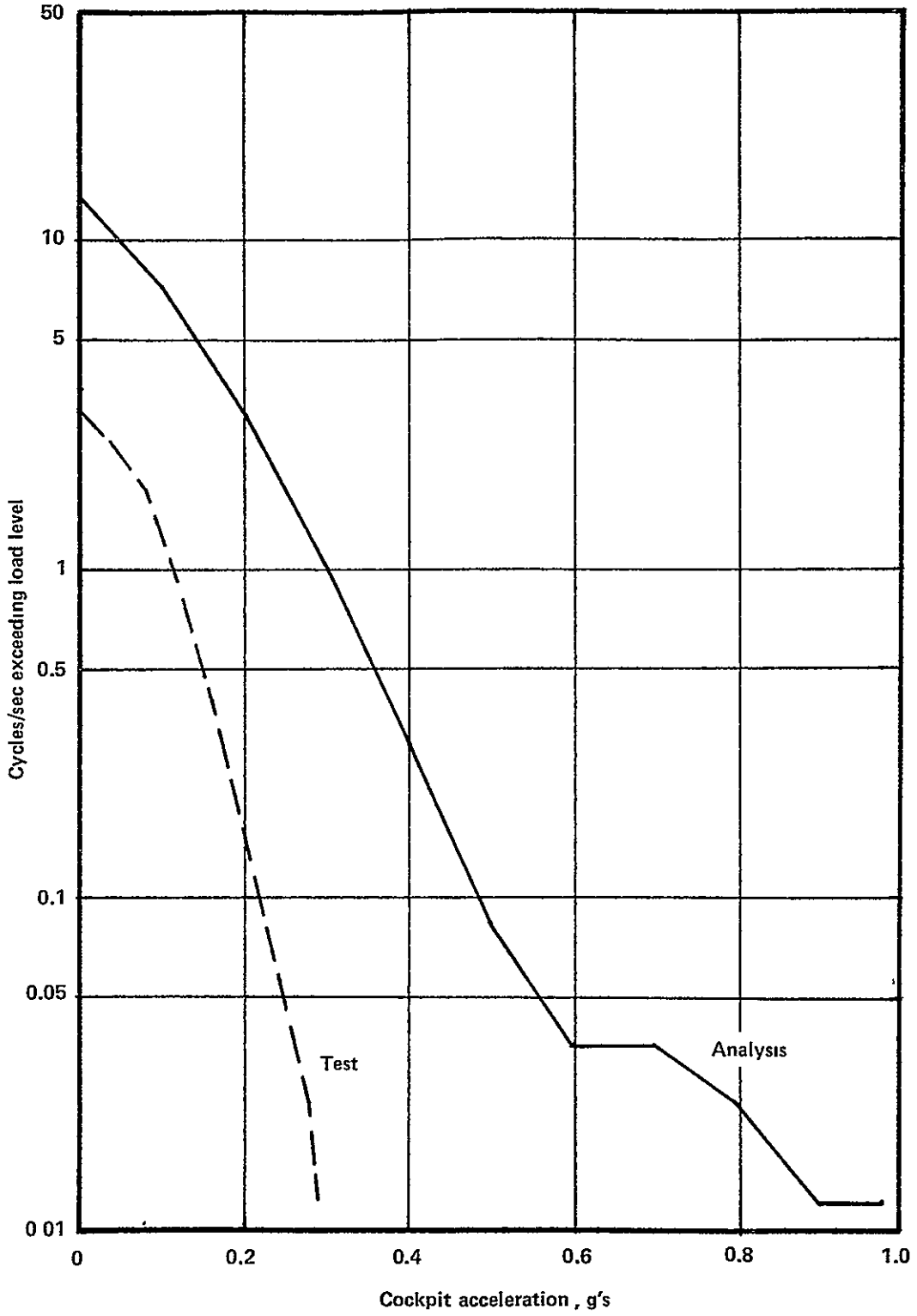

Figure 16.- Comparison of analytical and test results, cockpit acceleration, Test Series III.

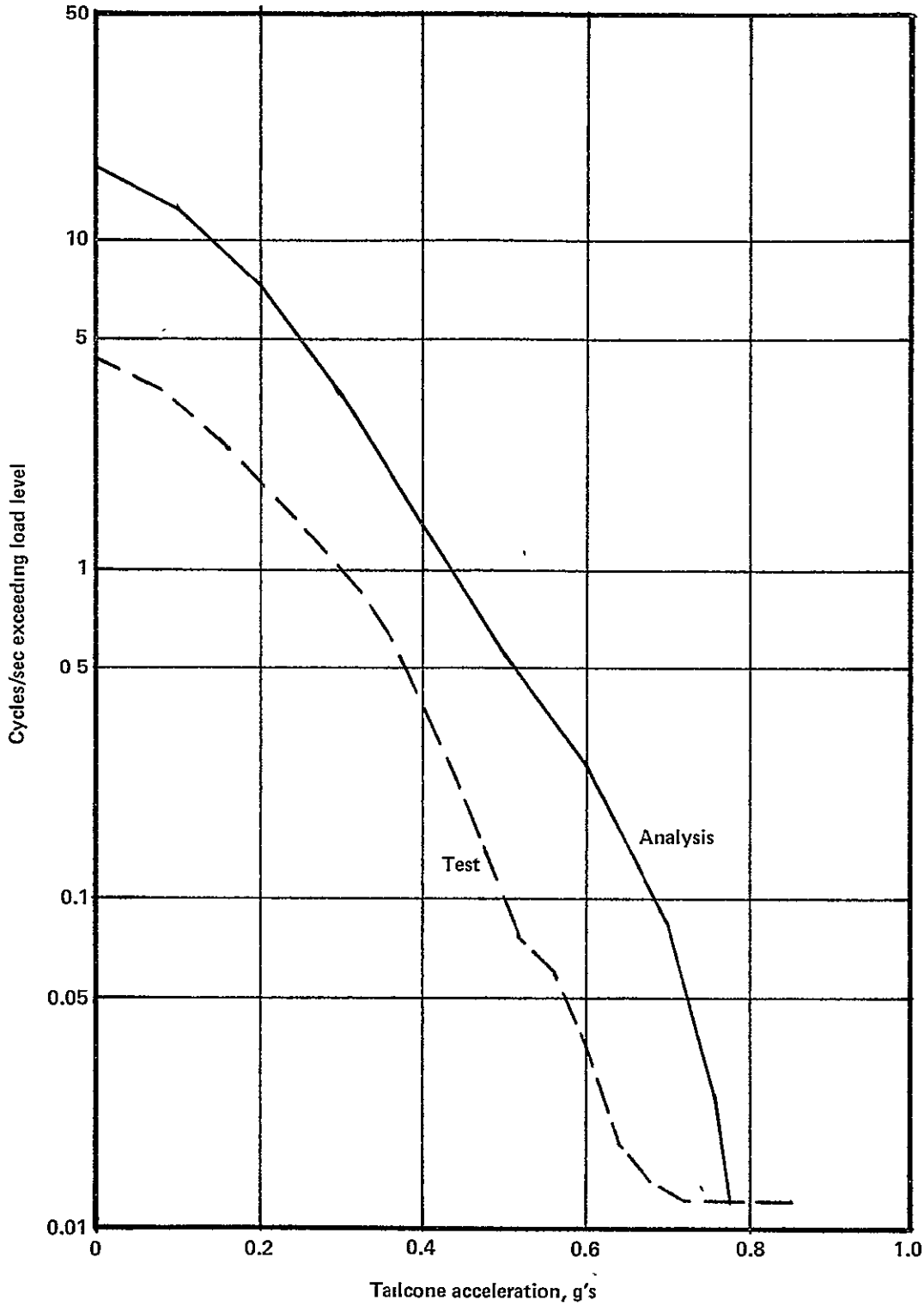

Figure 17. - Comparison of analytical and test results, tailcone acceleration, Test Series I.

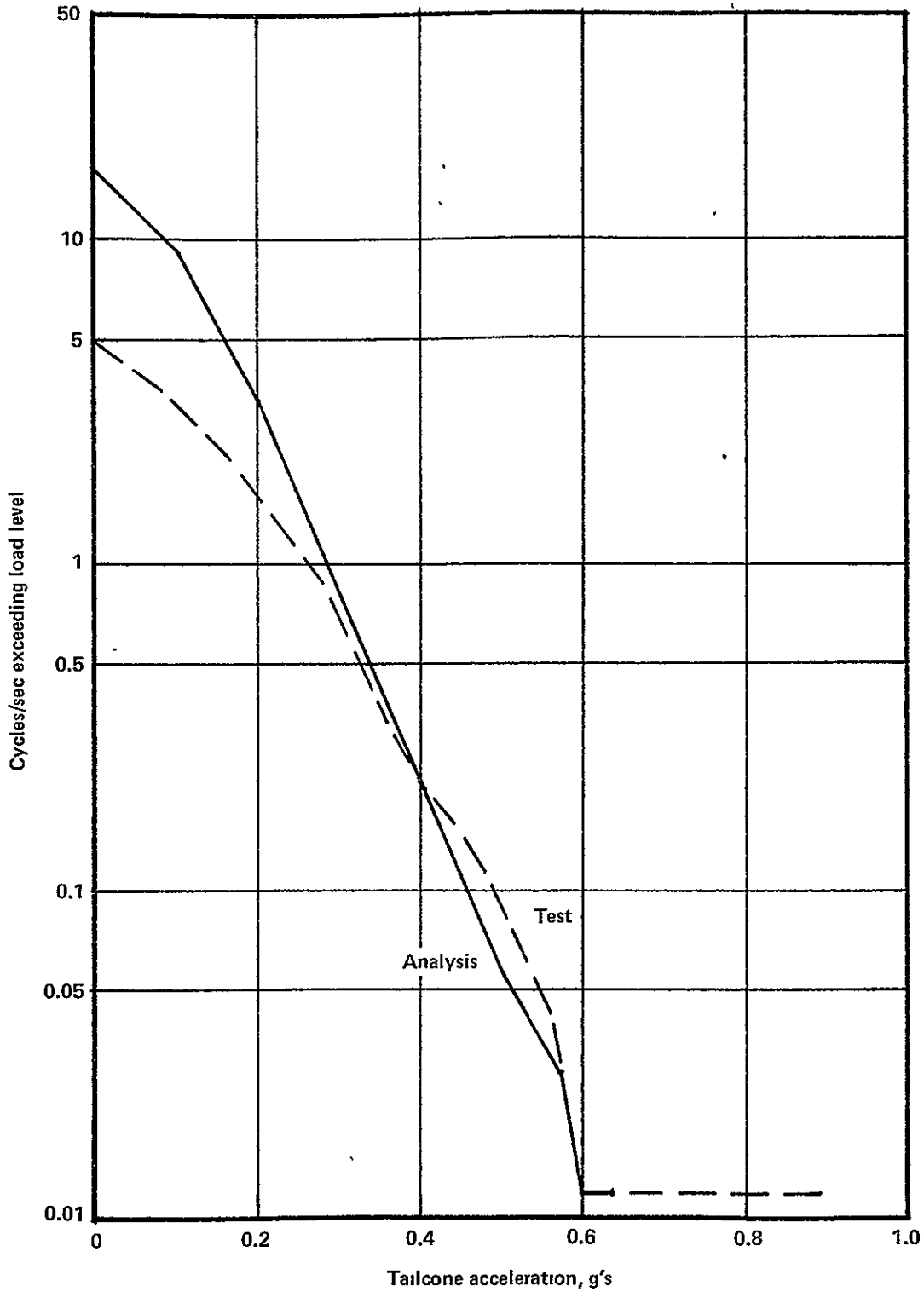

Figure 18.- Comparison of analytical and test results, tailcone acceleration, Test Series III.

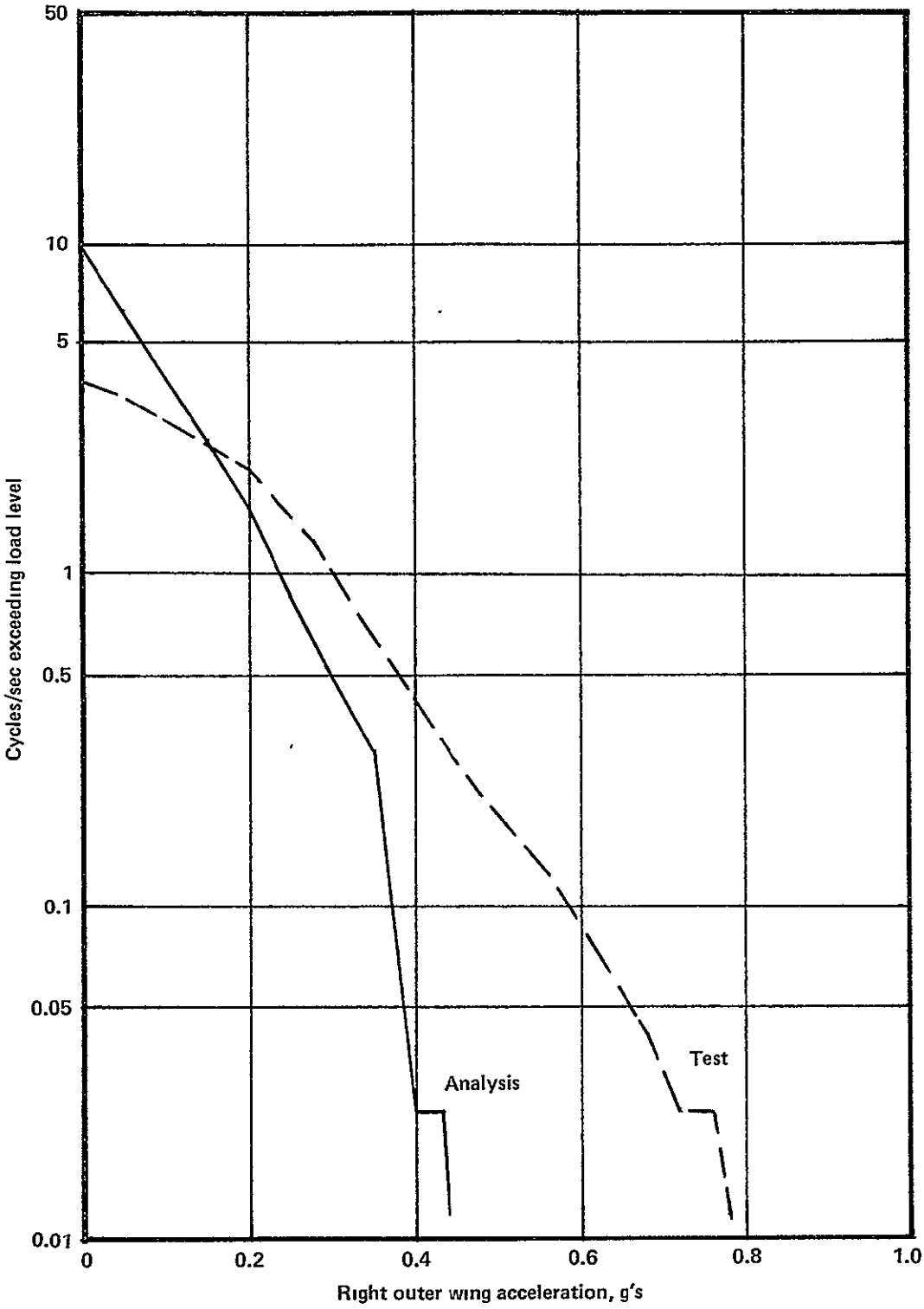

Figure 19. - Comparison of analytical and test results, right outer wing acceleration, Test Series I.

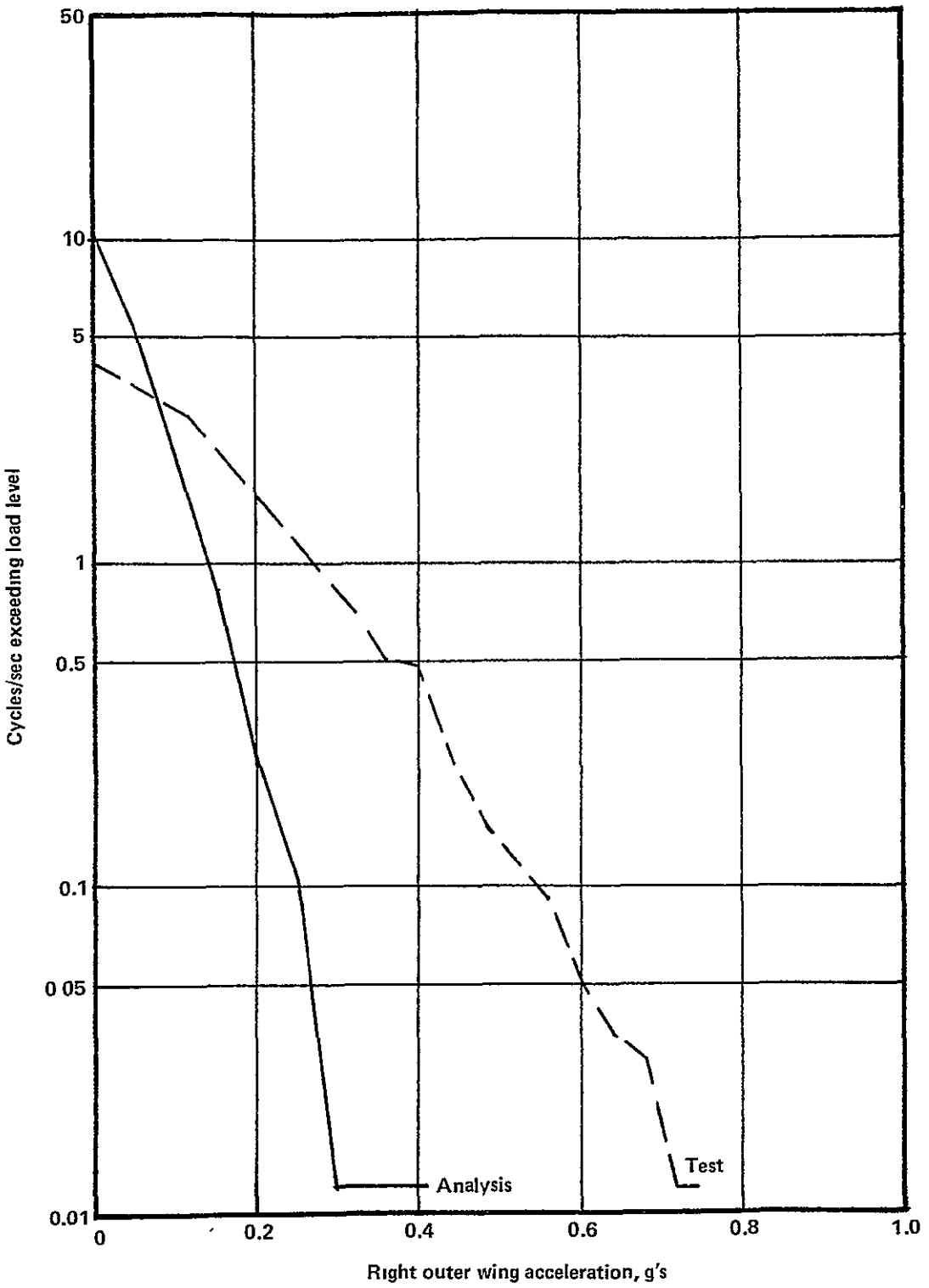

Figure 20.- Comparison of analytical and test results, right outer wing acceleration, Test Series III.

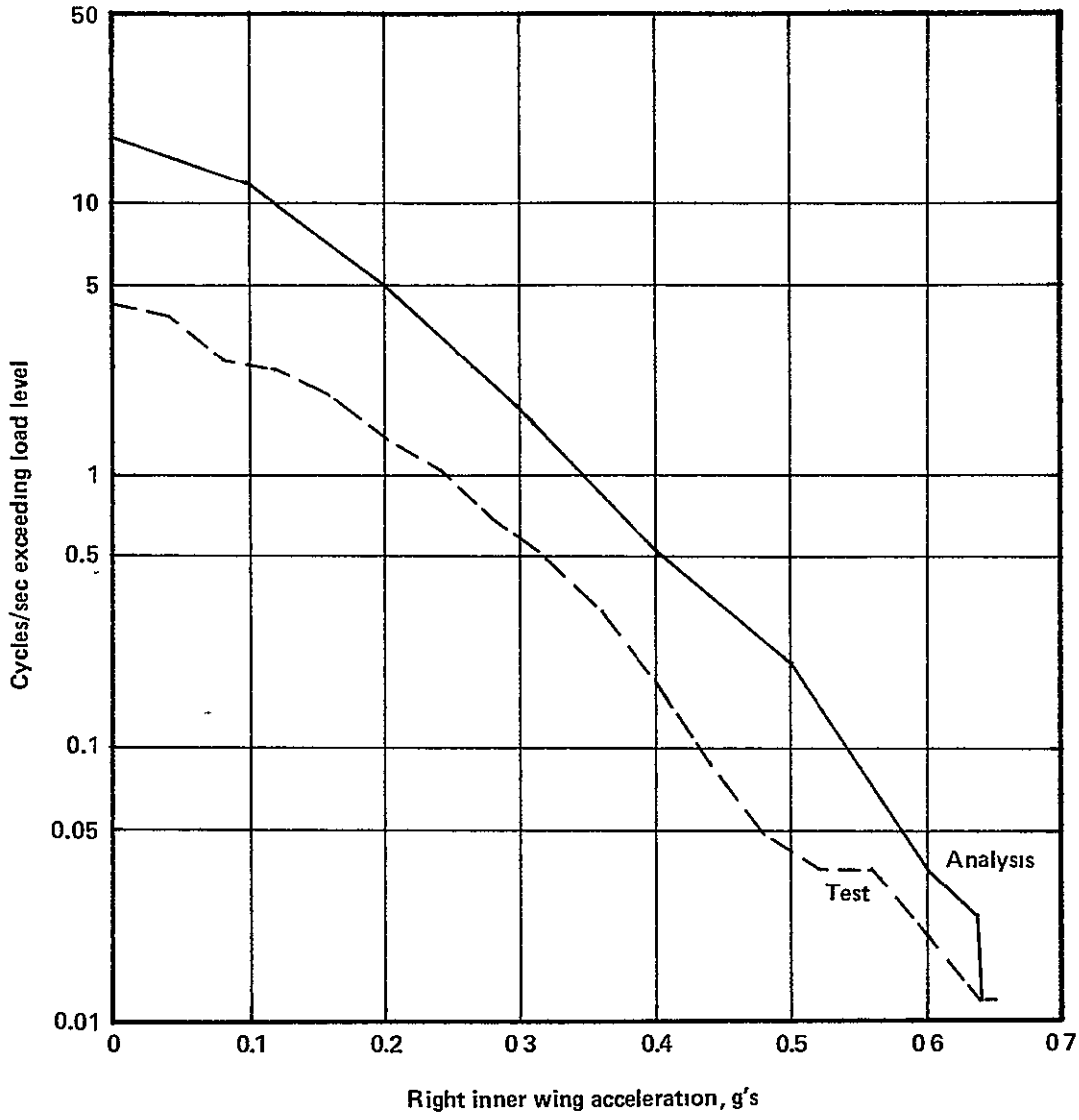

Figure 21.- Comparison of analytical and test results, right inner wing acceleration, Test Series I.

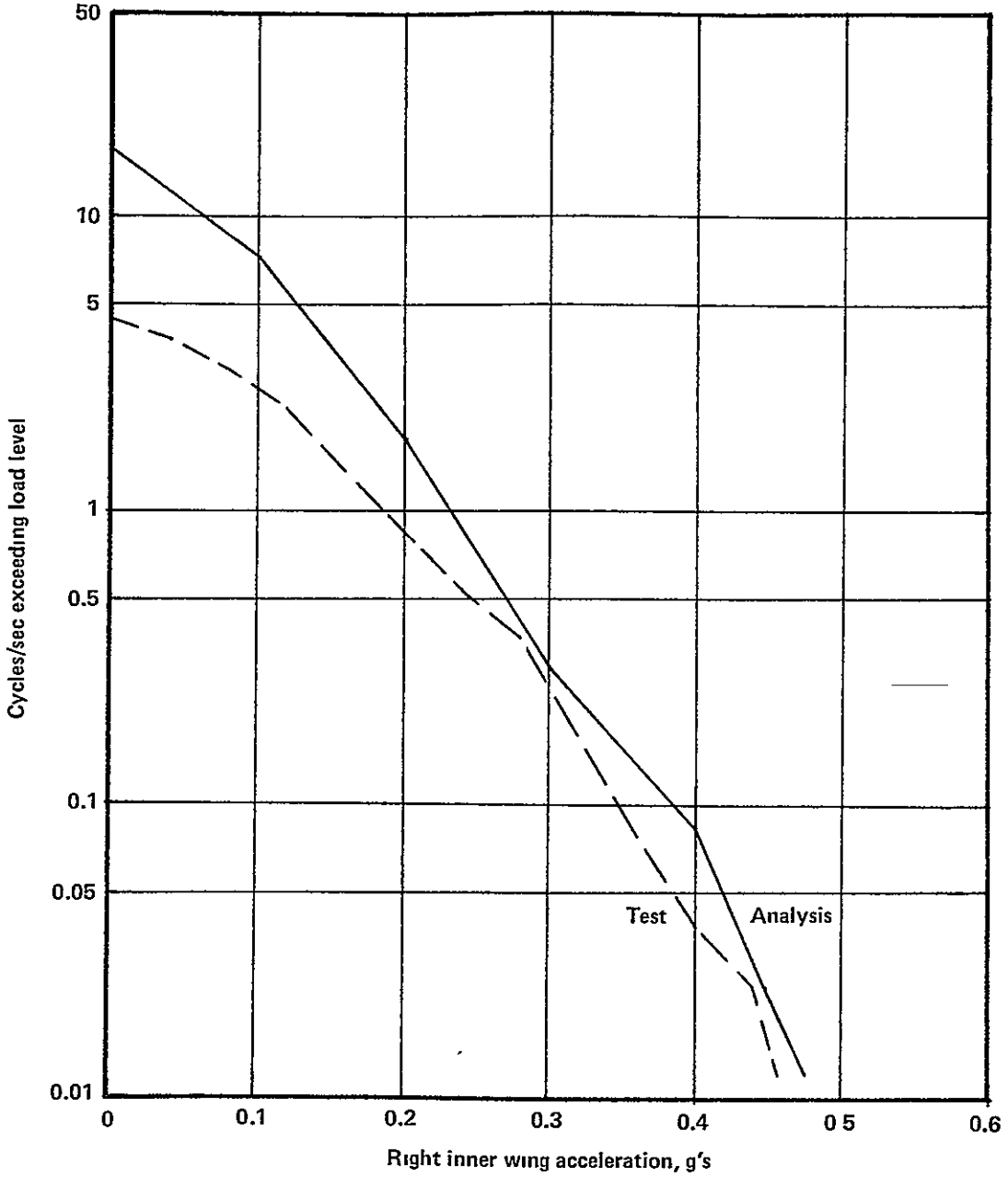

Figure 22.- Comparison of analytical and test results, right inner wing acceleration, Test Series III.

CONCLUSIONS

As a result of the test and analytical investigation of the performance of the dual-mode landing gear system on the YF-12A, the following conclusions are presented:

- The system as tested provides dynamic taxi response reductions of 25 percent at the cg and 30 to 45 percent at the cockpit. At the tailcone and right outer wing station, the responses are reduced less than 10 percent. At the right inner wing station, the responses are reduced 20 to 30 percent.

- The pilots commented that the dual-mode system resulted in a smoother ride during the constant velocity portions of the test runs, particularly at the higher gross weights.

- Analytical results based on a simple single-degree-of-freedom spring-mass-damper model of the airplane indicate that the observed test response reductions at the cg are of the magnitude that could be expected due to the softening of the main landing gears with the dual-mode system.

- Analytical results using a digital computer program to model the test taxi conditions yield excellent correlation with test data at the airplane cg, and good correlation at other locations on the airplane except the cockpit, which exhibits poor correlation between test and analysis.

- Analytical parameter variations indicate that the dynamic taxi responses at all locations on the airplane are very sensitive to the number of normal vibration modes used to model the flexibility of the structure.

APPENDIX A

DISCUSSION OF ANALYSIS VERSUS TEST RESULTS

Figures 13 through 22 of the main text represent the composite exceedances for Runs 2, 3, 4, 7 and 8. In order to investigate the effects of the flexible modes, Run 8 for Test Series I is analyzed with a varying number of flexible modes included in the analysis. A single run is used instead of the mix of five runs in order to reduce the computer analysis costs; Run 8 is chosen because it yields the largest loads for the majority of the response quantities. Analytical results are presented in Figures 23 through 27 for the following models.

- Rigid body
- First four flexible modes (Up to 7.5 Hz)
- First eight flexible modes (same as used for Figures 13 - 22) (Up to 15.6 Hz)
- First sixteen flexible modes (Up to 30.4 Hz)

In addition, each figure shows the test results. Since the results shown in Figures 23 through 27 are for run I-8 only, the degree of correlation between test and analysis differs from that shown in the main text, which is based on a mix of five runs. All flexible modes are symmetric. The modal damping used is shown in Figure 28. This curve is taken from Reference 2 and represents the structural damping values observed from various laboratory tests in which airplanes as a whole as well as various portions of airplanes have been excited.

Figure 23 shows that the analytical cg acceleration response increases significantly between the 4- and 8-mode solutions, and that the final 8 modes add very little to the response. Figure 24 shows that for the cockpit acceleration, only the rigid body and 4-mode solutions are reasonably close to the test results. The higher frequency modes continue to add to the cockpit response, with the full 16-mode analysis yielding a peak acceleration of nearly 2g. These high responses occur despite the very high damping values employed for the high frequency modes ($>20\%$ at 30 Hz).

In Figure 25, the tailcone responses correlate well with 8 modes, but the 16-mode results are again unrealistically high. In Figure 26, the right outer wing acceleration levels correlate well using the full 16 modes. However, it is felt that the inclusion of antisymmetric modes would add significantly to the responses at this location, so that once again the 16-mode solution would

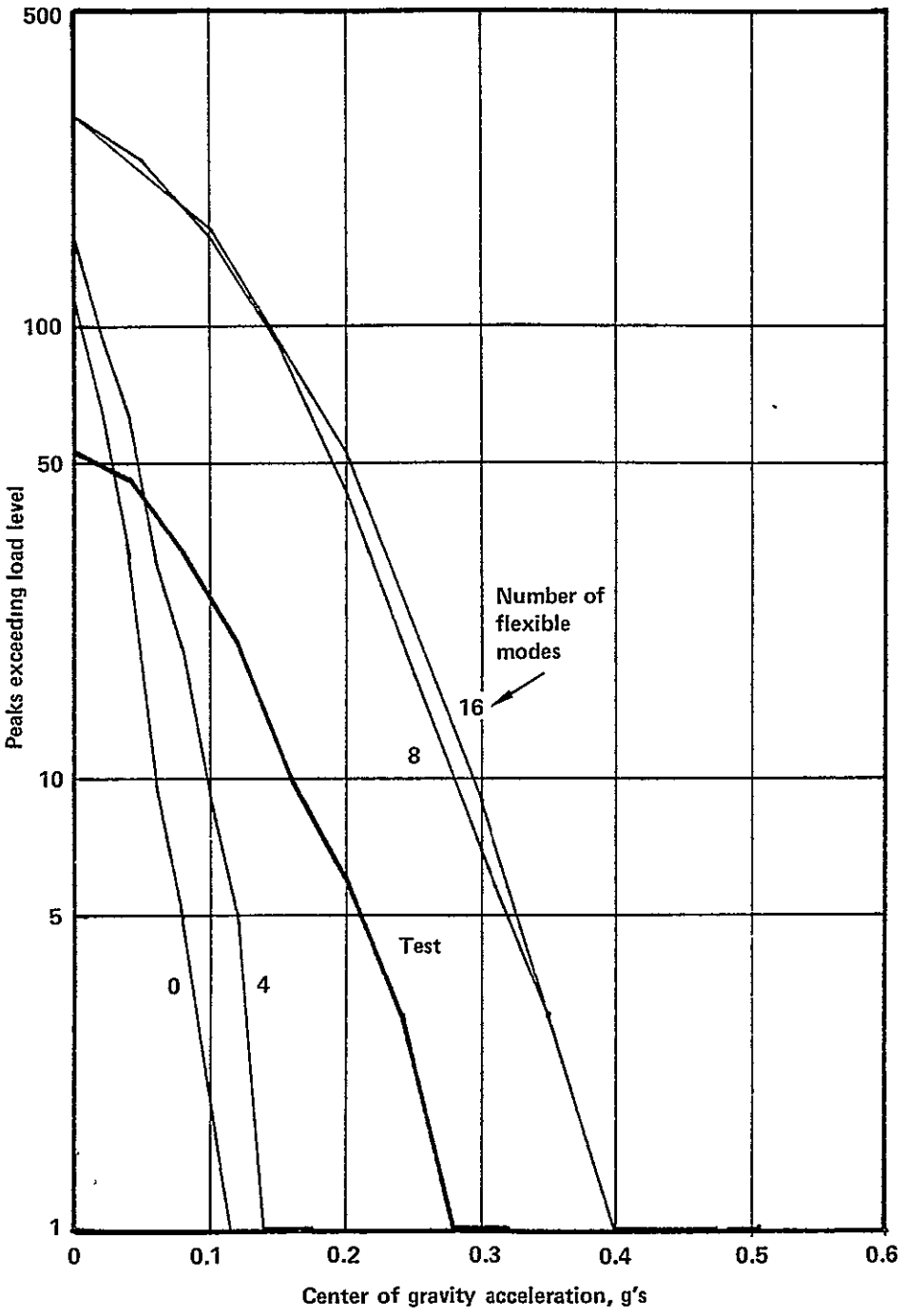

Figure 23.- Variation of analytical results with number of flexible modes, cg acceleration.

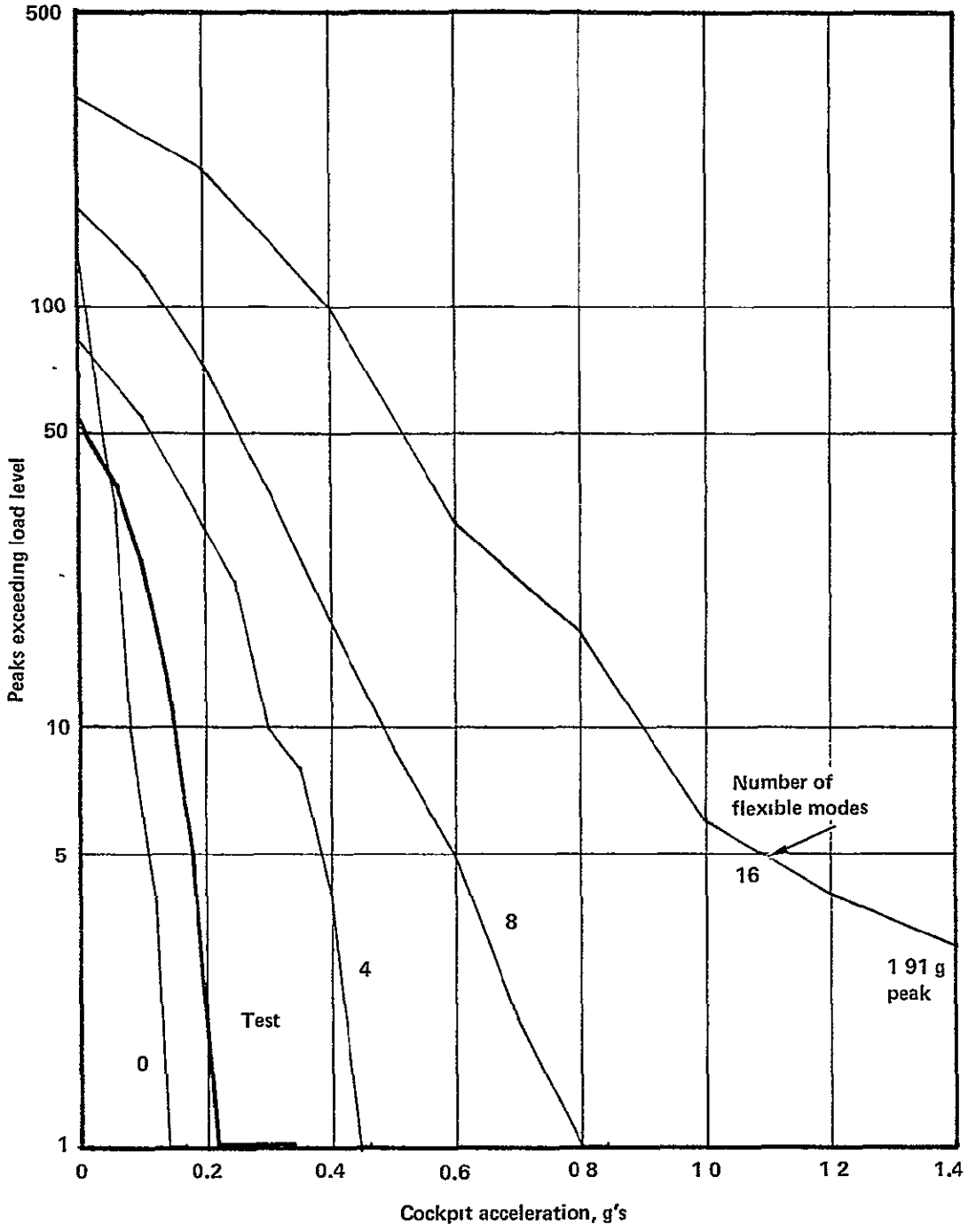

Figure 24.- Variation of analytical results with number of flexible modes, cockpit acceleration.

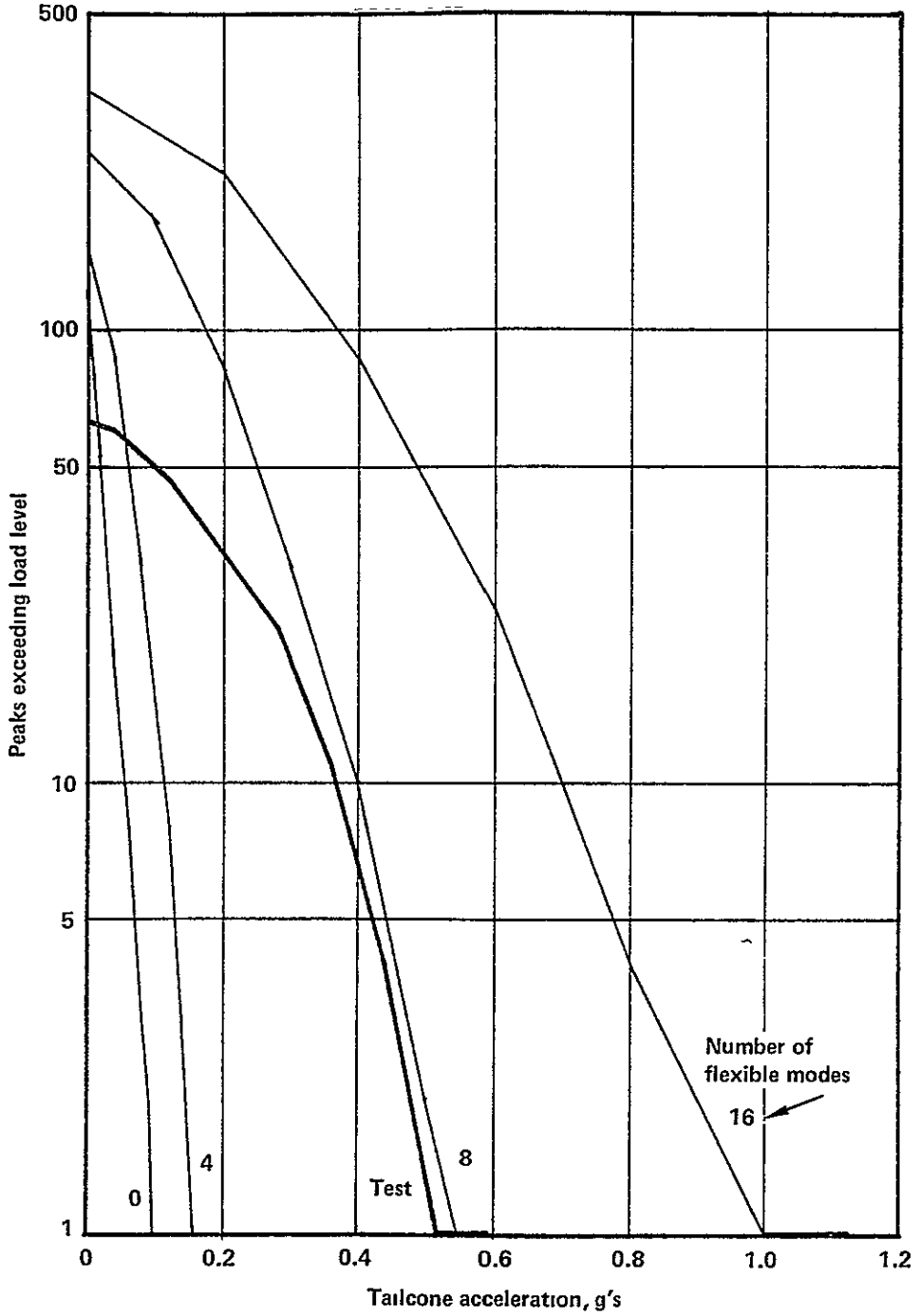

Figure 25.- Variation of analytical results with number of flexible modes, tailcone acceleration.

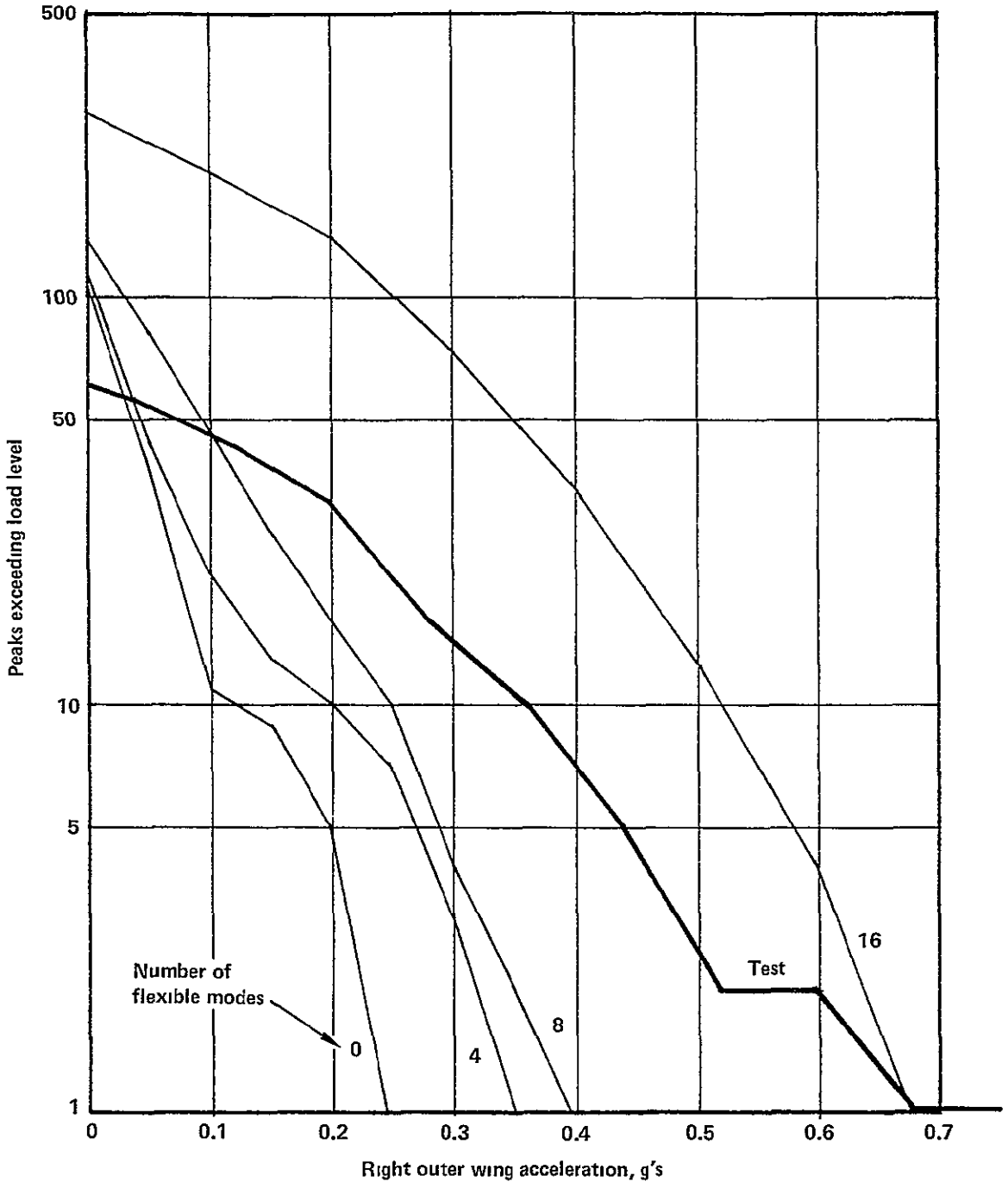

Figure 26.- Variation of analytical results with number of flexible modes, right outer wing acceleration.

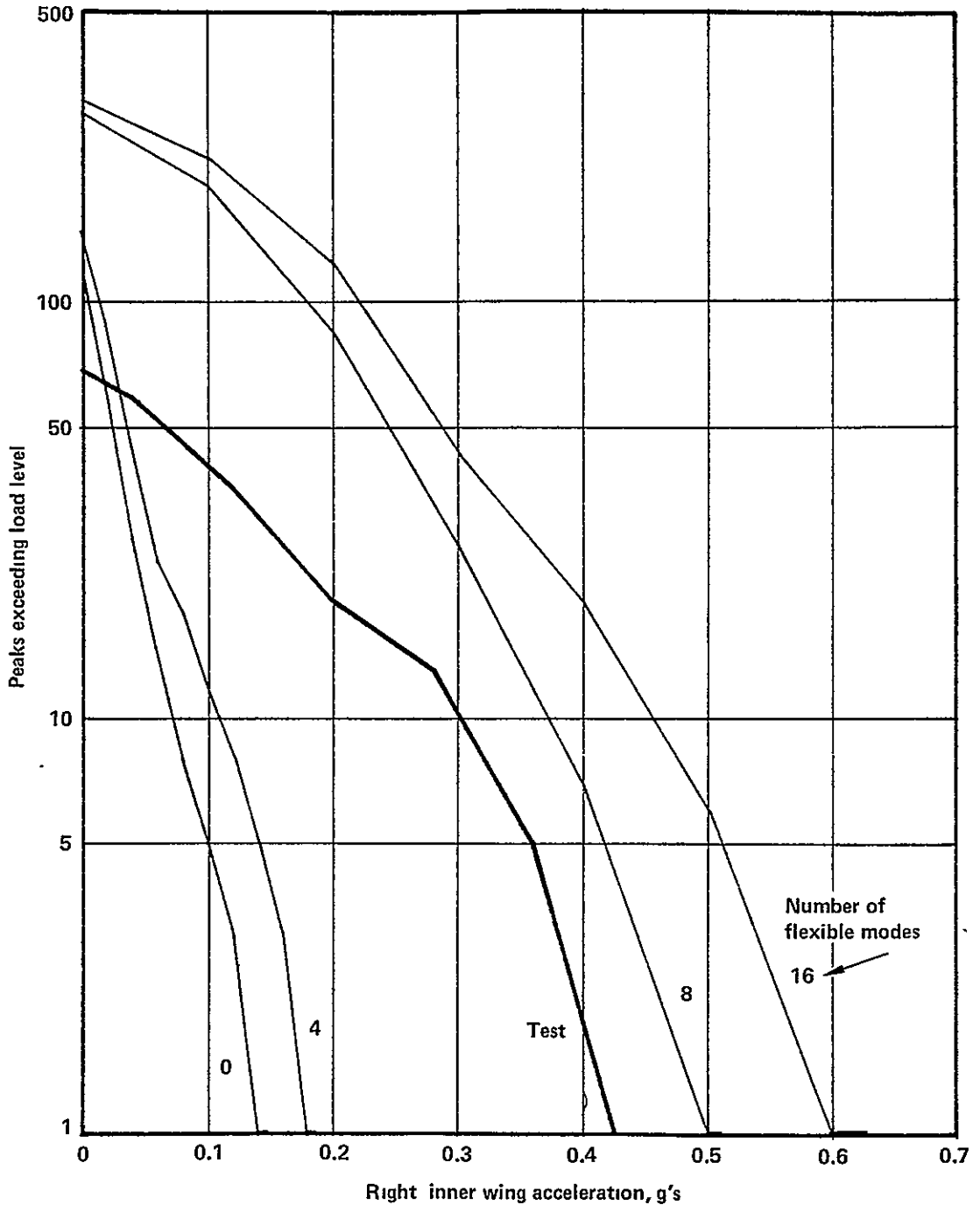

Figure 27. - Variation of analytical results with number of flexible modes, right inner wing acceleration.

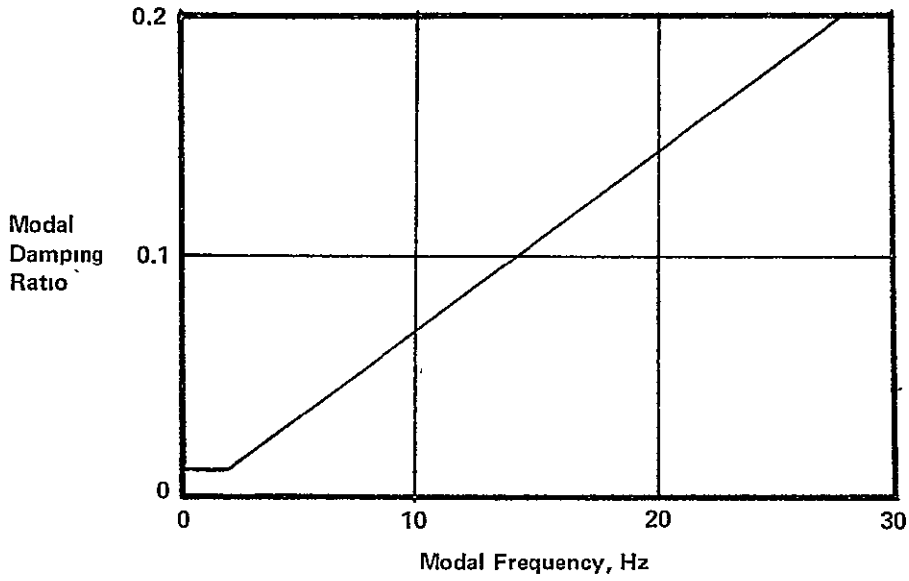

Figure 28. - Analytical modal damping

be unrealistically high. The right inner wing accelerations shown in Figure 27 correlate fairly well with 8 modes, and the 16-mode results are not too much greater than the 8-mode solution.

The results of Figures 23 - 27 tend to show that at interior regions of the airplane (cg and right inner wing), the first 8 flexible modes provide an accurate estimate of the vehicle structural response, and the final 8 modes do not add significantly to the acceleration levels. However, at the airplane's extremities (cockpit, tailcone and right outer wing), the higher frequency modes contribute significantly to the response levels.

The structural model used to develop the normalized vibration modes is relatively coarse in the forward fuselage region, with node points spaced about 12 feet apart near the cockpit. The total number of degrees-of-freedom in the elastic half-airplane model is 66. By comparison a typical elastic model for the L-1011 (half-airplane) contains 347 degrees-of-freedom. The L-1011 has about twice the wing area and fuselage length of the YF-12A, so that a YF-12A elastic model with a node-point density equivalent to the L-1011 model would have 347/2 = 173 degrees-of-freedom. The actual YF-12A model used has only 38 percent of this value. With the L-1011 analytical models, about 20 modes (up to 15 Hz) are actually used from the 347 degree-of-freedom model. If this same ratio were applied to the YF-12A model, only the first 4 flexible modes would be used. From these comparisons, it appears that there is justification for questioning the validity of the higher frequency modes derived from the YF-12A elastic model. For this reason, the correlation results presented in the main body of the report use the first 8 symmetric flexible modes.

The analytical results at all locations indicate a total number of peaks exceeding zero load level that is 2 to 4 times that of the test results. This results primarily from the fact that the test data plots used for peak counting are developed from digitized data which filters out high-frequency responses (above about 10 Hz). Examination of high-speed strip chart output of the test data indicates significant high-frequency contributions (18 - 30 Hz) to the acceleration history traces. Peak counts of this data would show a higher frequency of exceedance of zero load level, but no significant change at response levels above 0.2 g. Therefore, discrepancies between test and analytical frequencies of exceedance of zero load level are not considered significant, and the quality of correlation between test and analytical results is judged by the results at response levels above 0.2 g.

The results presented in this report are based on a model of the landing gears in which the rebound or extension damping constants are equal to the compression damping constants. For the nose gear, the calculated damping coefficients are 1.4 pound sec^2/in^2 during compression, and 25 pound sec^2/in^2 during extension. This large difference results in gear load histories that are unsymmetrical about the mean load, with large spikes resulting from high damping forces during extension. Plots of the test results do not show this unsymmetrical behavior of the nose gear loads. This fact tends to indicate that the theoretically calculated high rebound damping constant is not truly

effective on the airplane. In actual practice, a theoretically high damping constant can yield internal pressure high enough to cause cylinder expansion of sufficient magnitude to provide additional area for fluid flow. This reduces the effective damping constant actually achieved.

Examination of the Series I test data showing nose gear air pressure and strut position indicates that the nose gear was overpressurized by a factor of about 1.5 for the passive gear tests. This factor is included in the analytical results for Test Series I. For a given gear load, the gear stiffness (slope of nonlinear air load-deflection curve) is inversely proportional to the fully extended inflation pressure, so an overinflated strut provides a smoother ride than one with the nominal inflation.

Reference 4 presents the results of a correlation study performed by NASA-Langley to establish the validity of computer program FATOLA (Flexible Airplane Takeoff and Landing Analysis). Landing impact and rollout for the NASA YF-12A on Runway 22 at Edwards AFB are analyzed and compared with flight test data. The comparisons are limited to a 15-second period after initial main gear contact (nose gear touchdown occurs at 12 seconds), so only a limited amount of data representing three-gear taxiing is presented. The degree of correlation between test and analytical results is excellent for the overall airplane motions, such as pitch attitude, longitudinal cg acceleration, ground speed and the major strut compression of the main gears.

The responses to runway roughness inputs, however, as reflected in cg and cockpit acceleration histories, are not as accurately duplicated by FATOLA. Figures 6n and 6o of Reference 4 show that the computer simulation produces acceleration histories containing the proper frequency composition, consisting of a 2.5 Hz fundamental mode with a single dominant higher frequency mode at 18 Hz for the cg and 14.5 Hz for the cockpit. The magnitudes of the accelerations, however, are not accurately reproduced. For the maximum positive peaks, the analytical results for cg and cockpit are about 0.61 times the test results; for the maximum negative peaks, the ratio of analytical/test results is about 0.33. Figure 29 shows a comparison of test and analytical frequency of exceedance curves for cg acceleration based on Figure 6n of Reference 4. The analytically predicted gear force oscillations shown in Reference 4 also appear to be less than the corresponding test results.

The analytical models of the airplane and landing gear are essentially identical in the NASA and Lockheed computer programs. In addition, the same airplane flexible mode data is used. The discrepancies between test and analytical results of the two studies involving the same airplane and runway, coupled with the high degree of correlation between test and analysis achieved with the Lockheed dynamic taxi computer program modeling the L-1011 at Palmdale (Reference 5), suggest that the two correlation efforts may share a common problem. Although it is not possible with the available data to pinpoint the exact cause of the discrepancy between analysis and test results, the following items are considered to be potential contributors to the disparity:

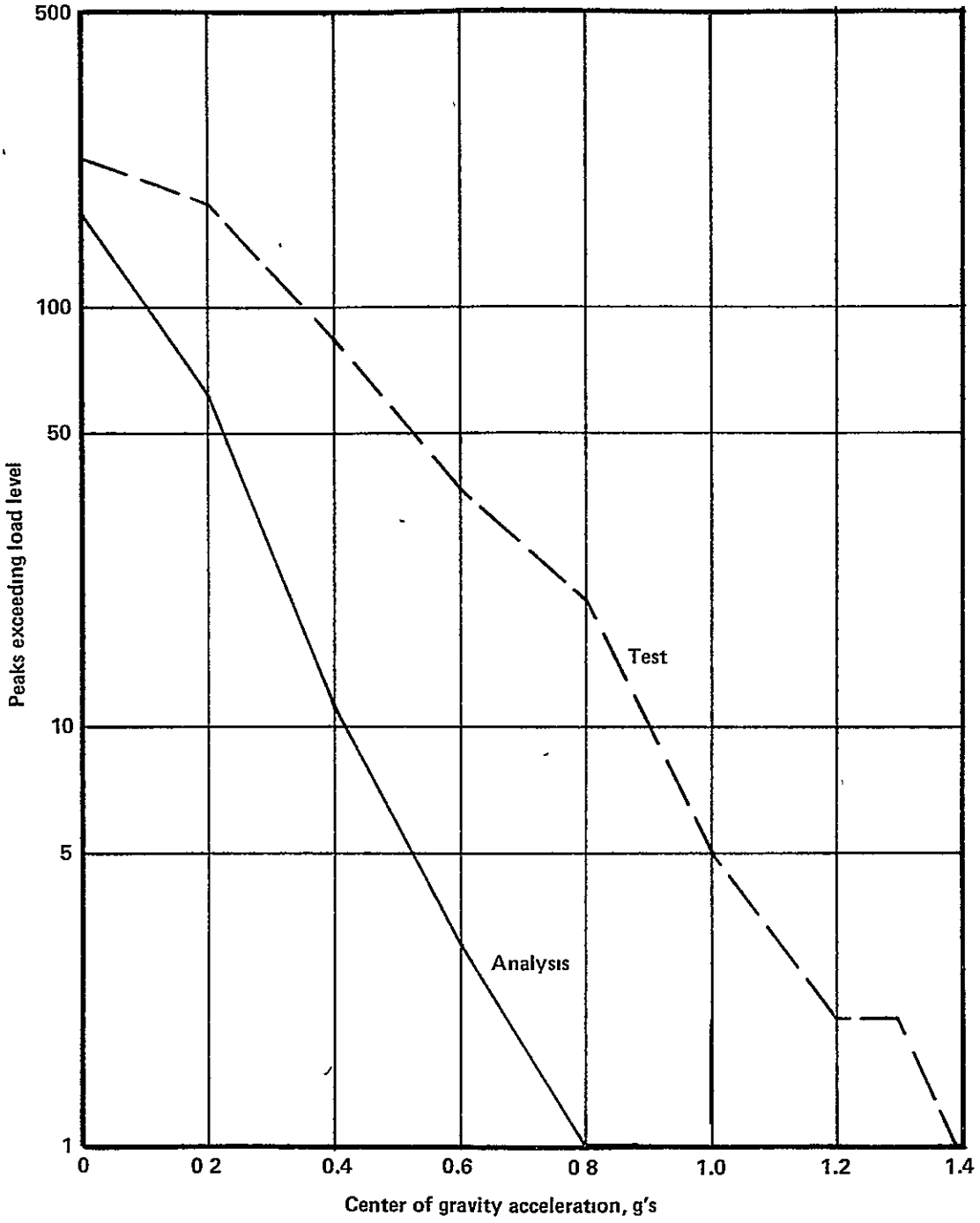

Figure 29. - Comparison of analytical and test results, center of gravity acceleration, NASA data from Reference 4.

- In Reference 4 it is mentioned that the airplane drifted as much as 15 feet off the runway centerline during the time period analyzed. In the current study certain of the runs were performed at lateral distances up to 25 feet from the centerline. These lateral offsets from the intended track may be sufficient to expose the airplane to surface unevenness that is significantly different from the measured profile data. Furthermore, the current runway surface profile may be different from that existing when the runway was surveyed.

- The calibration of the accelerometers may be inaccurate. In both studies the measured cockpit acceleration levels are below those at the cg. Normally, the reverse situation exists.

- Care must be taken to ensure that any filtering employed in the test data reduction process is compatible with the frequency response of the analytical model. The test data frequency response is determined by the basic response of the accelerometers, by any direct filtering employed (analog or digital), and by the time interval used to plot the data. The analytical frequency response is determined primarily by the number of flexible modes included in the analysis and by the integration time interval and by the plot interval.

- The accuracy of the analytical modal data strongly influences the response levels. In addition, antisymmetric modes can contribute significantly to response levels at locations removed from the airplane plane of symmetry.

- Proper servicing of the oil level and air pressures in each gear is essential. This is particularly evident in the current study because the function of the dual-mode adaptive gear is to alter the air curve by means of specific changes in air pressure and volume.

REFERENCES

1. Wignot, J.E., et al: Design Formulation and Analysis of an Active Landing Gear. AFFDL-TR-71-80, Volume 1, 1971.

2. Wignot, J.E., et al: The Development of Dynamic Taxi Design Procedures. FAA DS-68-11, 1968.

3. Anderson, D.L.: Hybrid/Digital Taxi Simulation. LR 25363, 1972.

4. Carden, H.D. and McGehee, J.R.: Validation of a Flexible Aircraft Take-Off and Landing Analysis (FATOLA). NASA TP 1025, 1977.

5. Lucas, M.W. and Storey, R.E.: Comparison of Airplane Measured with Theoretical Structural Loads, L-1011. LR 25141, 1972.

PAGE 48 INTENTIONALLY BLANK

1 REPORT NO	2 GOVERNMENT ACCESSION NO	3 RECIPIENT'S CATALOG NO.
NASA CR-144884		

4 TITLE AND SUBTITLE	5 REPORT DATE
TESTING AND ANALYSIS OF DUAL-MODE ADAPTIVE LANDING GEAR, TAXI MODE TEST SYSTEM FOR YF-12A	September 1979
	6 PERFORMING ORG CODE
7. AUTHOR(S)	8 PERFORMING ORG REPORT NO
Max A. Gamon	LR 28776
	10 WORK UNIT NO.
9 PERFORMING ORGANIZATION NAME AND ADDRESS LOCKHEED-CALIFORNIA COMPANY P.O BOX 551 BURBANK, CALIFORNIA 91520	11 CONTRACT OR GRANT NO
	13 TYPE OF REPORT AND PERIOD COVERED Contractor Report - Topical
12 SPONSORING AGENCY NAME AND ADDRESS National Aeronautics and Space Administration Washington, D.C. 20546	14 SPONSORING AGENCY CODE H-1100

15. SUPPLEMENTARY NOTES

NASA Technical Monitor: James M. McKay, Dryden Flight Research Center

16 ABSTRACT

A combined test and analytical program was conducted to determine the effectiveness of a dual-mode adaptive landing gear system in reducing the dynamic response of an airplane during ground taxiing. Results are presented of dynamic taxi tests of the NASA YF-12A research airplane at Edwards AFB. Analytical results using a digital computer program to simulate the test conditions are discussed. Test and analytical results are shown both for the basic airplane and for the airplane modified to incorporate a ground-test version of the dual-mode landing gear system.

17. KEY WORDS (SUGGESTED BY AUTHOR(S))	18 DISTRIBUTION STATEMENT
dynamic taxi landing gear active gear YF-12A	Unclassified - Unlimited STAR category: 05

19. SECURITY CLASSIF. (OF THIS REPORT)	20. SECURITY CLASSIF. (OF THIS PAGE)	21 NO. OF PAGES	22 PRICE*
Unclassified	Unclassified	56	

*For sale by the National Technical Information Service, Springfield, Virgina 22161